CONCEPT IMPLEMENTATION OF SMALL SCALE ACTIVE CONTROL VOLUMETRIC FLOW RATE METER

by

Patrick Lambie

A thesis submitted to the Faculty and the Board of Trustees of the Colorado School of Mines in partial fulfillment of the requirement for the degree of Master of Science (Petroleum Engineering).

Golden, Colorado

Date: _____

Signed: _____
Patrick Lambie

Signed: _____
Dr. Jorge Sampaio
Thesis Advisor

Golden, Colorado

Date: _____

Signed: _____
Dr. Erdal Ozkan
Professor and Head
Department of Petroleum Engineering

ABSTRACT

Despite many shortcomings, methods claiming to measure volumetric flow rate (VFR) have been widely applied to delta flow integration on land drilling operations. Currently, the industry uses sensors, paddles, Coriolis meters and other flow meters, to approximate volumetric flow rate. While none of these devices actually measure volumetric flow rate, they are used on land drilling rigs every day to indicate flow rate and provide critical data for volumetric calculations. The true volumetric flow rate of returned drilling fluid and cuttings to surface is generally unknown because industry lacks a reliable method to measure volumetric flow rate. The purpose of this research is to identify a flow meter capable of measuring volumetric flow rate reliably.

The Active Control VFR Meter operates off the mass continuity principle using a progressive cavity pump PCP to maintain a fluid level of returns in a cone bottom tank, filled from the return line. The lab-tested small scale Active Control VFR Meter demonstrates the ability to identify changes in VFR in real time before increasing or decreasing the pump output to measure the volumetric flow rate of the mud return line. The Active Control VFR Meter's ability to quickly identify small changes in flow rate, expand its ability to double as an early influx/loss detection meter. Fluid density is calculated at the Active Control VFR Meter using tank pressure sensor measurements. PCPs are known for their ability to pump a wide range of multiphase media typical to drilling operations. The testing and implementation of this VFR meter has the potential to change how future land drilling rigs measure return fluid flow rate, early influx detection, and measure VFR with gpm accuracy.

TABLE OF CONTENTS

LIST OF FIGURES

LIST OF TABLES

CHAPTER 1

INTRODUCTION

Every year billions of dollars are spent managing well control related issues encountered while drilling. As the US land rig fleet has modernized over the past decade, the industry has done little to develop or adopt a more accurate method to measure the return flow rate on land drilling rigs. Return flow rate is an essential yet undervalued parameter frequently overlooked and misused. The return flow rate would otherwise help indicate well control issues before they fully progress. Properly identifying the wellbore return flow rate is vital to maintaining proper well control during drilling operations. The problem with properly identifying the return flow rate involves the puzzling methodology behind existing flow rate sensor technology still used today.

The main concern associated with drilling fluid measurements is the variability in flow rate and pressure throughout the drilling operation. Flow rate sensor readings frequently produce inaccurate results. Most of the current flow rate technology calculates flow rate based on the measurement of pressure, RPM, paddle displacement, or wave transmission timing. The problem with using these measurements is the wide range of limitations that adversely disrupts the method of measurement.

The Coriolis flow meter remains one of the more highly regarded mass flow rate sensors currently offered within the industry. They are critical to the success of offshore operations because of the risks associated with taking a massive influx and the costly non-productive time (NPT) of an offshore rig. The problem with the widespread implementation of the Coriolis flow meter is that they are typically reserved for offshore rigs and high profile extended reach land drilling rigs due to relatively high capital costs (upwards of $300k). Since the cost associated with litigation following a well control related event is comparatively high; the demands for affordable, early influx/loss detection systems continue to grow. As a result, influx detection systems continue to improve in reliability and influx detection time.

The purpose of this research is to use the principle of mass continuity to develop an automated small-scale VFR meter that reliably determines the volumetric flow rate and fluid density. Understanding why and where current flow rate meters fall short, is critical when

developing a superior VFR meter. A superior system is one that instantly and autonomously identifies a small fluid influx while reliably determining the density and change in volumetric flow rate. Therefore, the objectives to study in this research involve the following: First, investigate the application of mass continuity principle and directly measure VFR. Second, investigate and determine methods to quantify VFR meter behavior in a dynamic system. Third, define actions necessary to resolve factors that hinder VFR meter performance. Studying these objectives will advance the research necessary to identify the plausibility of measuring flow rate with a volumetrically efficient method. An autonomous VFR meter would improve rig efficiency and overall safety of drilling operations when compared to the current flow rate sensors on the market.

CHAPTER 2

TECHNICAL REVIEW

Methods used to measure fluid properties while drilling have changed very little in the past 40 years. Flow paddle indicators, pit volume sensors, ultrasonic flow sensors, and Coriolis meters are limited in scope because they cannot provide the required accuracy and repeatability where multiphase fluid conditions exist. Spitzer (2010) argues that current technology claiming to measure volumetric flow rates only truthfully measure parameters such as; sound pulse transient time, distance, force, mass flow rate or pressure. These parameters are used to calculate and infer flow rates that lead to high noise and error. The Coriolis flow meters claim accuracy and repeatability for mass flow rates but require expensive software and calibration to estimate the volumetric flow rate. Flow rate sensors have remained relatively simplistic despite the large technological advances in other areas of the industry. Today, the demand for faster, more accurate, and more affordable flow sensors and early influx/loss detection sensors have increased to reduce NPT and maximize drilling efficiency.

2.1 Flow Rate Measurement Methods

It is critical to detect an influx or loss circulation event as it forms in the wellbore because the intensity of either event will increase in severity the longer each event remains uncontrolled or undetected. The most effective method to detect an influx or loss in a closed loop drilling system is by measuring delta flow (outflow minus inflow). Speers and Gehrig (1987) explain how delta flow is the fastest method to identifying a change in flow rate while drilling. The following subsections discuss the different types of flow rate measurement sensors currently used to measure in the industry today.

2.2 Mud Pump Stroke Counter

This method counts the number of strokes to determine the volume of fluid pumped by multiplying strokes by the volume of fluid displaced per stroke. True pump output is the pump efficiency factor multiplied by the calculated rate. This method is capable of determining the volumetric flow rate of a VFR Meter but is not reliable due to limitations. These limitations include uncertainties in the true efficiency factor, wear of cylinder, and seal, and slow response time due to the long period required to cycle one stroke. Schafer et. al. (1992) finds that typical

mud pump efficiency range between 86-96%.

2.3 Pump Rotary Speed Transducer

This method uses an optical encoder to determine the revolutions per minute with a high level of accuracy (287 times a stroke). True pump output multiplies the pump drive shaft RPM by the pump volume, and pump efficiency. Limitations of this method include arbitrary efficiency percentages and poor volumetric efficiency.

2.4 Magnetic Flowmeter

This method generates a magnetic field through a full wetted pipe and measures the distortion in magnetic flux when aqueous fluid flows through the pipe. The associated distortion of flux corresponds to fluid velocity, the multiplied by flow area to determine the fluid flow rate through the flow meter. This equation provides great accuracy if the fluid type is electrically conductive. Limitations can only work with water based drilling fluids, cannot use at high pressure, with fluids containing 10-20% gas, and this flow sensor is expensive (still half as much as an equally sized Coriolis system). Schafer et. al. (1992) finds that typical accuracy found with magnetic flowmeters is between 2-9%. Solids settled out in a return line can disturb flow (plug flow lines) and reduce accuracy.

2.5 Doppler Ultrasonic Flowmeter

This method uses ultrasonic pulses traveling through a pipe and then receives an offset signal known as the Doppler shift. The shift is a quantified function of the sound speeds upstream and downstream a flowing fluid. The total flow rate is the fluid velocity multiplied by the flow area. Interference created by electrical and mechanical environments (found on most drilling locations) limit accuracy and reliability. Schafer et. al. (1992) finds that normally the rate measured with this flow meter is 35% greater than the actual flow rate.

2.6 Flow Paddle

This method is one of the most common flow rate indicators used on land rigs to measure either flow or a percentage of flow. The spring-mounted paddle deflects upward with increasing fluid force related to the amount of flow. The amount of paddle deflection relates to impact force between the fluid and face of the paddle. Since impact force is a function of height and velocity, it is also a function of flow rate. Limitations include poor repeatability and accuracy. Significant

changes in fluid viscosity and fluid weight negatively affect this method. Schafer et. al. (1992) finds that error in flow rate identified with this meter is 15% greater than the actual flow rate.

2.7 Acoustic Level Meter

This method uses an acoustic sensor to emit a pulse above open flow and then receives the return pulse. The echo time of the fluid is proportional to the distance between the fluid level and the transducer. Changes in temperature, the density of air (or gas), and settled out cuttings in the return line influence accuracy. Schafer et. al. (1992) discusses limitations including susceptibility to noise interference and that acoustic level meters typically indicates an 8% greater than the actual flow rate.

2.8 Rolling Float Meter

Geothermal wells popularly use the rolling float meter to determine loss circulation while drilling. The system employs rolling a counterbalanced float that rides and slides on the fluid level in the return line. The float arm connects to a potentiometer, indicating the angle and the height of the float. Magnets added to float identify the relationship between rotation and linear fluid velocity. Changes in viscosity, density, or base depth of cuttings do not affect reliability or accuracy. The error identified with this method ranges within a max deflection of ±2% from the actual flow rate.

2.9 Coriolis Flow Meter

The most advanced method of determining the return line mass flow rate commonly used on offshore platforms is the Coriolis mass flow meter. Norman (2011) explains that the Coriolis device has no moving parts and can take up essential room on the rig depending on the size and orientation of both the rig and the Coriolis. Flow Solutions Blog (2016) summarizes the Coriolis system and explains how the fluid forced through a semi-loop or u-tube induces vibrations due to slight changes in mass flow momentum. This method measures mass flow rate by identifying the vibration frequency offset and using the amplitude of the vibration to calculate density. Livelli (2010) identifies the problems with the significant head pressure required to force the return fluid through the flow meter and the costly software required to clean up noise on the output. Speers and Gehrig (1987) identify the requirement to integrate the Coriolis Flow Meter output signal to the rig's system to display mass flow rate. These systems are expensive, therefore, only offshore or land rigs operating near the Arctic Circle normally use this method to

determine mass flow rate. The sensors in a Coriolis flow meter calculate the real-time mass flow rate of the return line pumped through it. Alarms are set to notify crews of a significant change in fluid density or mass flow rate so that appropriate actions mitigate the issue as soon as possible. This system is also the only system to calculate the density and mass flow rate before the shakers remove cuttings from the return fluid. This is the best point to measure flow rate and density because of the conservation of mass and volume. The offset observed is the vibration frequency recorded at each end of the u-tube, used to calculate the difference in mass flow. The amplitude of the vibrational frequency defines density. The fundamental problem with this meter is the system requires full flow to operate the Coriolis system's pipes or the flow rate cannot be determined due to lack of rate and therefore inertia.

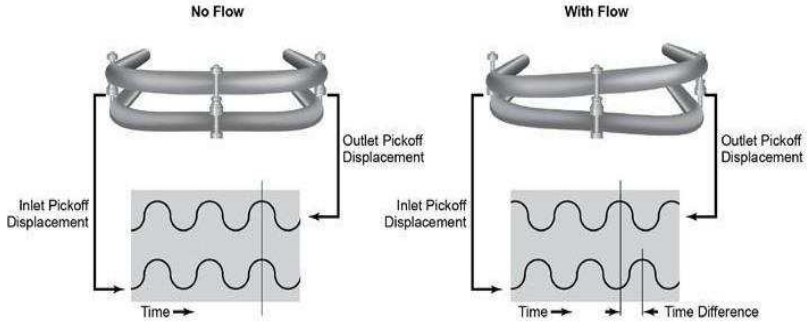

Figure 2.1 Visualization showing how the Coriolis system works.

2.10 Pit Volume Totalizer

Multiple floats measure the height of the drilling fluid in the return tank. This method measures the time to fill up a known volume tank and calculates the average flow rate. Several (up to 32) tanks can be used at one time to facilitate quasi-continuous flow measurement. However, the system has low sensitivity to quick changes in flow rates and for intermittent changes. This method is more accurate than the manual dipstick method used to measure collected drilling fluid volume. However, if a loss of circulation event occurs at the same time an influx develops, it is possible for the density of the fluid at the return line to decrease while maintaining the same physical volume. It would be impossible to know that the bottom hole pressure is decreasing until the driller or derrick man manually measures the density every 30-minutes. Within 15 minutes of the 30 minute window, an influx could have ample time to develop and migrate up the wellbore. Undetectable, the influx could make it past a point in the well to where it would become impossible to mitigate with well control.

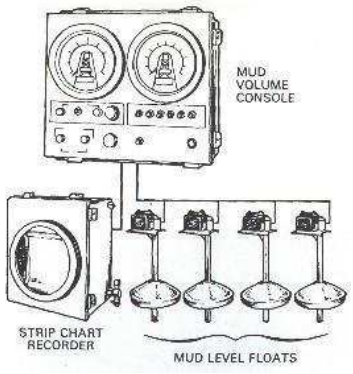

Figure 2.2 Visualization of pit volume totalizer.

2.11 Influx Detection

An influx is an unintentional increase of fluid into the borehole of a well. This occurs when the pressure exerted by the column of fluid is less than the pore pressure at a depth of the influx. As stated by Ahmed et al. (2015), the three conditions that must occur for an influx to occur in open hole are:

1. *Formation pore pressure must be greater than the fluid pressure in the borehole.*
2. *The formation permeability must be sufficient to allow flow into the borehole.*
3. *Pore fluid must have low enough viscosity to flow.*

One of the most critical components of a successful drilling operation is the accuracy and consistency of the well's drilling fluids program. One of the primary functions of drilling fluid is to properly manage bottom hole pressure while drilling. This creates a hydrostatic pressure barrier between the high pressures at the bottom of the wellbore and the normal, safe working pressures at the surface. Depending on the in-situ fluid within the formation when an influx occurs. The formation can inject fresh water, brine (high salinity liquid), hydrocarbons, dry gas, wet gas, or a combination of these fluids into the annulus of the wellbore. Depending on the size of an influx, the drilling fluid's ability to maintain bottom hole pressure control is hindered. If the bottom hole pressure continues to decrease, the formation may inject another influx into the borehole.

The earlier an influx is detected and shut-in; the easier is to control and remove the influx. Therefore, any system that can detect the subtle increase in fluid volume could aid in the reduction of influx intensity.

2.12 Early Influx Detection Methods

Fraser et.al. (2014) discusses the early influx detection methods by highlight the importance of two key performance indicators as they relate to influx:

1. *How long does it take to positively identify an influx?*
2. *How long does it take to respond to an influx once the identification is made?*

The first indicator identifies the human response time required to make a decision. The second indicator is an evaluation of human detection, analysis, and physical response time to shut-in the well. Today, neither of these reactions should identify key performance indicators relating to an influx. With the right early influx detection system, the human delay should appear negligible because the system should answer or identify any question regarding the identification of an influx. The main benefit to using an early influx detection system is to have another tool on location advising a proper procedure to implement and eliminate the guesswork involved by reducing human error. Fraser et. al. (2014) addresses one of the issues by implementing inflow-outflow Coriolis sensors to improve detection time. However, the Coriolis sensors cannot detect flow at the wellhead when the drill string is out of the hole, and they are limited with low flow rates. Additionally, a volumetric flow rate sensor would alleviate several issues as Fraser et. al. (2014) alluded to, when discussing the requirements needed to use the Coriolis meter. Fraser et al. (2014) also identifies limitations such as the high head pressure requirement, the software required to fix the noise, and lack of personnel with knowledge involving proper installation.

It is important to think about return flow rate with respect to the pump flow rate to identify when an external factor changes the total volume of the circulation system. Fraser defines the ratio of return flow rate to pump flow rate as the Flow Rate Ratio (FRR) or delta flow. During normal drilling operations, the flow rate pumped into the well should equal the return flow rate out of the well. Changes in the FRR provide valuable insight into the dynamic downhole environment. An increase in the FRR is indicative of an uncontrolled influx into the wellbore, also known as an influx. A decrease in the FFR is indicative of lost circulation.

CHAPTER 3

RESEARCH METHODOLOGY

Problem-solving research methodologies identify the design parameters necessary to characterize system performance in this study.

3.1 Principle of the VFR Meter

The principle of mass continuity states that, in a control volume (CV), the rate of mass entering the CV minus the rate of mass leaving the CV equals the rate of mass accumulation in the CV. If the mass in the discussion is that of incompressible fluid, or a fluid with very low compressibility (as the case of drilling fluids) the mass in this statement can be replaced by volume since mass equals density multiplied by volume. Therefore, the mass continuity statement now reads, the flow rate entering a CV (flow-in) minus the flow rate leaving the CV (flow out) equals the rate of fluid volume accumulation in the CV.

If one can measure the flow-out and the rate of fluid volume accumulation, then the flow-in is immediately calculated. If the rate of fluid volume accumulation is zero, the flow-in then equals the flow out. Equation 3.1 and 3.2 support this:

$$q_i - q_o = \frac{dV}{dt} \tag{3.1}$$

$$q_i = q_o + \frac{dV}{dt} \tag{3.2}$$

q_i = Flow into velocity tank, gpm

q_o = Flow-out of the pump, gpm

V= volume of fluid inside the velocity tank, gal

dV/dt = the rate of accumulation inside the tank, gpm

For a fluid accumulated in a vertical cylinder of cross-section area A, volume V is given by Ah, where h is the level of the fluid in the cylinder. Therefore, the expression:

$$\frac{dV}{dt} = A\frac{dh}{dt} \tag{3.3}$$

A system using a cylindrical accumulator with a constant cross-section area (velocity tank) can supply a volumetric pump (e.g. a progressive cavity pump) to determine the flow rate out of the system. The flow rate out is obtained by multiplying the pump speed (RPM) by the pump factor (the volume pumped by each revolution of the pump rotor). The rate of fluid volume accumulation, in principle is obtained by measuring the fluid level velocity (*dh/dt*) multiplied by the cross-section area A of the tank.

An appropriate sensor measuring the fluid level over time can numerically obtain the fluid level velocity. These parameters feed an appropriate controller, which dictates the pump RPM and consequently the flow rate out.

It is worthwhile noting that the introduction of cuttings to the drilling fluid at the bit does not affect the total return flow rate at the surface. The volume of cuttings introduced to the drilling fluid is exchanged with hole volume as the bit drills through the rock. While the fluid density increases with the introduction of cuttings, the flow rate of the return fluid remains constant.

In summary, using a volumetric pump by adjusting the rotation speed of the pump rotor can control flow out. The velocity tank with a fixed cross-sectional area measures the rate of accumulation.

3.2 Assumptions

Using a submersible pump to simulate return fluid flow to surface is valid with the following assumptions:

- *The compressibility of drilling fluid is so minimal that it is an incompressible fluid and therefore volume can replace mass in the principle of mass continuity.*
- *The influx of cuttings entering the wellbore does not affect the return flow rate at the surface as the volume of rock replaces the drilling fluid at an equal rate.*
- *The pressure acting on the progressive cavity pump is so small that slippage does not occur and the pump factor maintains 100% volumetric efficiency.*

- *Mechanical efficiency of the motor in the system is 100% or otherwise negligible.*
- *The wellbore fluid temperature was ambient (68 degrees Fahrenheit) to reduce the cost of the flow-loop test system.*
- *The wellbore fluid chemical composition and corrosiveness is equal to that of fresh water to reduce the cost.*
- *The pressure of the fluid entering the velocity tank is ambient since an open trough supplies the return flow to the flow rate sensor's velocity tank.*
- *The current technology limiting the maximum progressive cavity pump output was ignored for testing purposes.*
- *The flow rate from the wellbore would never be greater than the maximum flow rate output of the progressive cavity pump.*

3.3 Design of Test Flow Loop

The test flow-loop design involves two main systems identified in Figure 3.1.

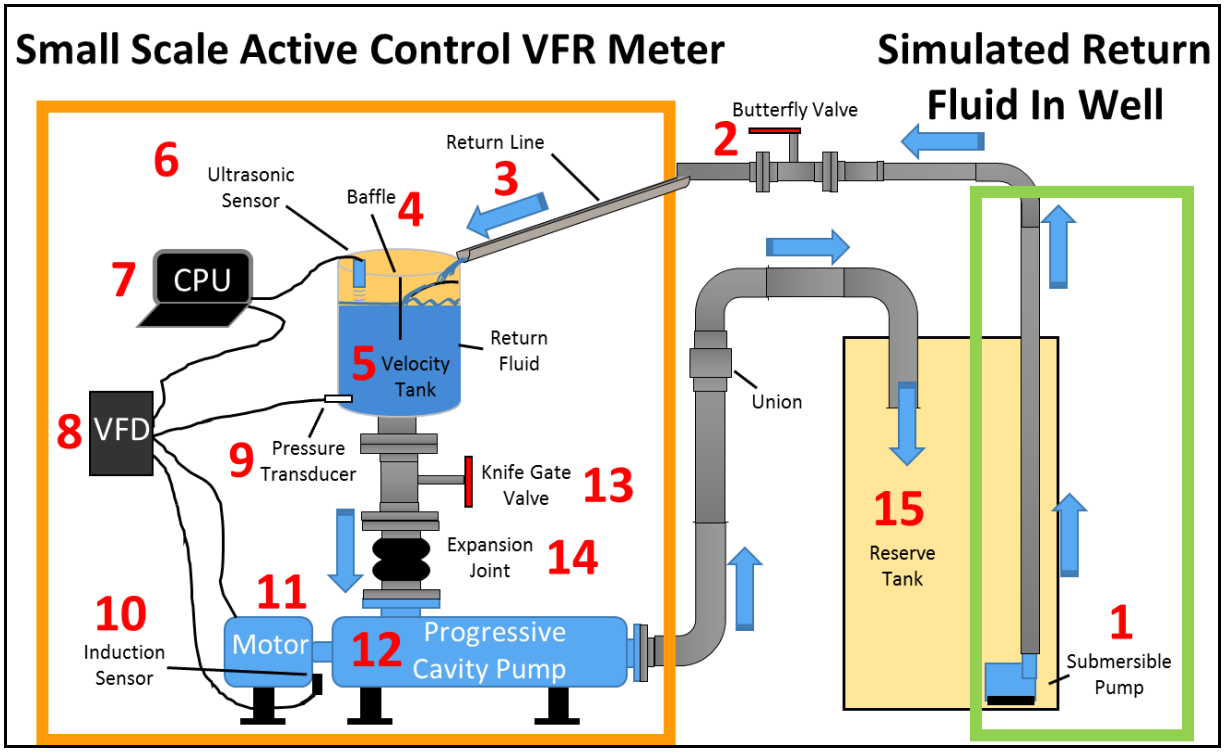

Figure 3.1 Small scale Active Control VFR Meter design.

The following describes the components of each of the main systems identified and the components that facilitated flow-control for testing.

Components Simulating Fluid Flow Returning from Well:

1. *Submersible Pump*
   The submersible pump operates at a fixed flow rate of 36.59 gpm. This fluid flow represents drilling fluid as it flows up the annulus to surface.

Components for Lab Testing Purposes Only:

2. *Butterfly Valve*
   The butterfly valve is not a real component of the rig flow loop or the VFR Meter and only facilitates flow-control for lab testing. The butterfly valve varies the flow rate from 0.0 gpm to 36.59 gpm. This permits the option to change the flow rate, simulating an influx or loss event during testing.

Components for the Volumetric Flow Rate Sensor on Surface:

3. *Return Line*
   Normally, the return line transfers the drilling fluid from the bell nipple to the shale shakers. However, when implemented, the volumetric flow rate sensor is placed between the bell nipple and the shale shaker. Therefore, the return line, when used with the volumetric flow rate sensor, only transfers drilling fluid from the bell nipple to the top of the velocity tank.

4. *Baffle/ Fluid Dampener*
   The fluid dampener slows the velocity of the fluid flow into the velocity tank to avoid high-velocity turbulent flow from creating level measurement noise in the velocity tank. Air may mix with the drilling fluid if the fluid flow is turbulent and may decrease the fluid density. The baffle reduces inaccuracies in the measurement of the fluid level measurements by reducing the fluid velocity as the flow enters the velocity tank.

5. *Velocity Tank*
   The velocity tank contains the drilling fluid slowed and redirected by the baffles to determine fluid level height in the tank and determines fluid density using a pressure transducer at the bottom of the tank.

6. *Ultrasonic Sensor*

   The ultrasonic sensor measures the distance between the sensor and the surface of the drilling fluid to find the fluid height in the mud tank. The ultrasonic sensor also finds the rate at which the drilling fluid level changes in the velocity tank.

7. *CPU (Central Processing Unit)*

   Sensor data sent to a computer running LabVIEW uses a proportional integral (PI) controller to determine the appropriate voltage needed to change the pump output and maintain a target fluid level in the velocity tank.

8. *VFD (Variable Frequency Drive)*

   The VFD acquires a signal from the CPU and modulates the frequency output sent to the motor to change the RPM of the pump and maintains a constant fluid level.

9. *Pressure Transducer*

   The waterproof pressure transducer measures the pressure at the bottom of the velocity tank to calculate the density of the fluid.

10. *Induction Sensor*

    When a small metal washer (within 7 mm of sensor head) taped to the rotating pump rotor disrupts the electrical field of current at the head of the sensor, it sends a 5 V digital signal to the NI DAQ where the signal relates to an equivalent pump shaft RPM. The pump's discharge flow rate is determined multiplying the RPM by the 0.2 gal pump factor. When the velocity of the fluid level is zero, the flow rate entering the velocity tank equals the PCP flow rate.

11. *Motor*

    An induction motor reduced by a gearbox transfers the appropriate RPM needed at the pump shaft to produce the flow rate necessary to maintain the fluid level in the velocity tank.

12. *(PCP) Progressive Cavity Pump*

    The PCP used for this project has a maximum flow rate 36.59 gpm. The volumetric efficiency of the pump is essentially 100% due to low pressures. The PCP has an integrated anti-dry run thermocouple sensor installed in the stator's housing. If the pump runs dry while operating, the anti-dry run sensor will detect the increase in the

pump rotor temperature and shut down the pump. The pump factor for this PCP is 0.2 gallons per rotation.

13. *Knife Gate Valve*

    The 4.0 in. PVC gate valve installed in the 4.0 in. flanged stack to add an extra level of flow control should a welded PVC joint or gasket fail. The knife valve prevents the fluid from draining out of the system.

14. *Rubber Doublesphere Expansion Joint*

    A 4.0 in. rubber expansion joint prevents motor induced vibrations from disrupting the fluid level inside the velocity tank. It critical to preserve system accuracy by maintaining a flat (non-dynamic) fluid level with minimal wave action to improve the ultrasonic sensor accuracy and to reduce motor ramp cycling caused by noisy data.

15. *Reserve Tank*

    This tank has a capacity of 125 gallons and acts as both the output (shale shaker) and the fluid reservoir at the bottom of the wellbore (provides the submersible pump fluid to discharge as return flow).

The Active Control VFR Meter could interrupt the return line and reside in a small footprint in between mud tanks and the drilling rig. See Figure 3.2 for an illustration identifying the placement of the Active Control VFR Meter on a land drilling rig location.

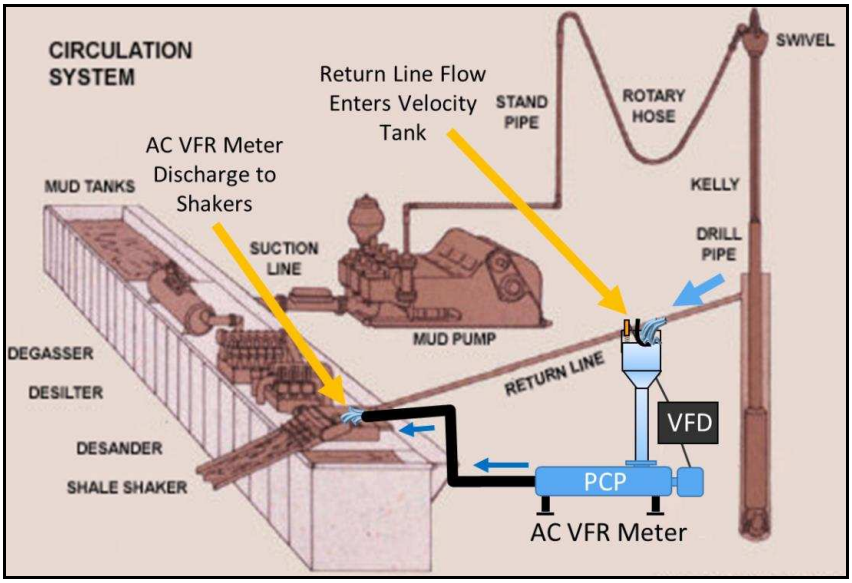

Figure 3.2 Active Control VFR Meter operates in the drilling flow loop.

See Figure 3.3 for the Active Control VFR Meter used to conduct this study.

Figure 3.3 Active Control VFR Meter used to perform research.

3.4 LabVIEW Logic

This research utilizes National Instruments (NI) hardware and LabVIEW software to design a sophisticated user interface and control system. This NI (2017) system runs autonomously in real-time for rapid hardware and systems control. Testing the sensors wired to the NI DAQ verify the appropriate signal output and to calibrate the sensor. The block diagram shown in Figure 3.4 illustrates, the PI (proportional-integral) controller logic utilizing local and global feedback for rapid controller response. The proportional controller controlled the fluid level in the velocity tank. The integral controller in this system, modulated, sends voltage to the plant (VFD, motor, and pump) to control the desired fluid level velocity changes (K_i/s). The controller uses proportional gain (K_p) to monitor the fluid level in the tank and integral gain (K_i/s) to control fluid level velocity.

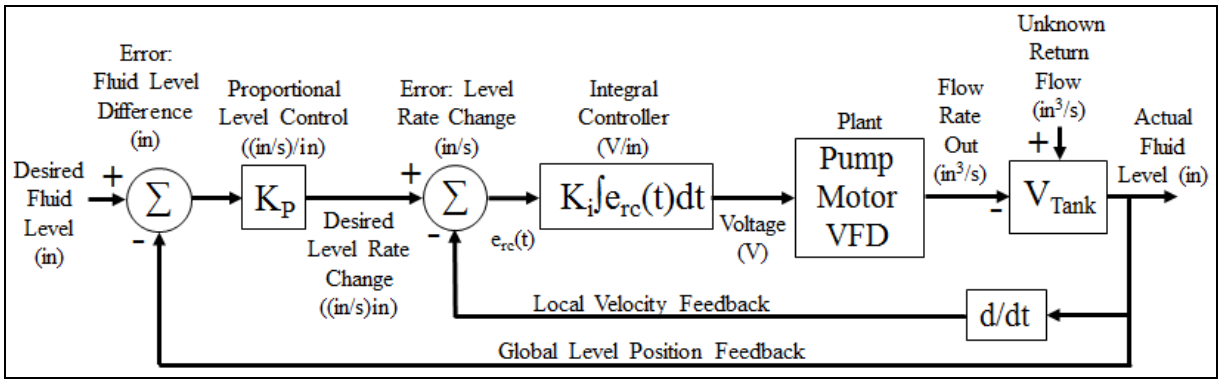

Figure 3.4 Block diagram of the PI system controller.

A logic test of several PID (proportional-integral-derivative) control types, determines controller logic effectiveness within the mechanical system. The first two PID control methods tested did not perform as desired and produced significant integral windup as Avery, P. (2017) discusses. Manually tuning the proportional and integral gains optimize and dampen the system.

CHAPTER 4

DATA ANALYSIS RESULTS

Tests determine the Active Control VFR Meter's response time, accuracy, and reliability to dynamic fluid flow rate simulations. See Table 4.1 for a schedule of tests performed.

Table 4.1 Active Control VFR Meter Test Schedule

Active Control VFR Meter Test Schedule						
Test #	Initial Flow Rate (gpm)	Initial Fluid Level (in.)	Control System Gain Settings		Change in Volume (gal) or Flow Rate (gpm)	Time Influx/Loss Introduced (s)
			Ki (V/in.)	Level Kp ((in./s)in.)		
Simulation #1: Single Fixed Volume Influx - Gradually Added						
Test #1	18.0	13.5	5.0	0.05	1.0 gal	10.0 s
Test #2	18.0	16.5	4.5	0.05	1.0 gal	10.0 s
Test #3	6.0	16.5	3.0	0.02	0.5 gal	10.0 s
Simulation #2: Fixed Flow Rate Influx - Immediate Increase						
Test #4	6.0	15.0	3.0	0.02	4.4 gpm	Instant
Test #5	6.0	15.0	3.0	0.04	5.9 gpm	Instant
Test #6	6.0	16.0	3.0	0.02	9.4 gpm	Instant
					4.4 gpm	Instant
Test #7	24.8	16.0	2.8	0.02	0.8 gpm	Instant
Simulation #3: Fixed Flow Rate Loss - Immediate Reduction						
Test #8	36.6	13.5	3.5	0.02	- 4.4 gpm	Instant
Test #13	21.3	13.5	3.5	0.05	- 4.4 gpm	Instant
Test #14	21.3	13.5	3.5	0.05	- 4.4 gpm	Instant
Simulation #4: Increasing Flow Rate Influx - Slowly Introduced						
Test #9	6.0	13.5	3.5	0.04	4.4 gpm	80.0 s
Test #10	6.0	13.5	3.5	0.05	4.4 gpm	60.0 s
Test #11	6.0	13.5	3.5	0.05	4.4 gpm	60.0 s
Test #12	6.0	13.5	3.5	0.05	4.4 gpm	120.0 s

Since the PCP output would determine the flow rate into of the system, a pre-test was required to validate the 0.2 gal/rev pump factor provided by the PCP manufacture. If the PCP pump factor did not match the specification provided, then the real gal/rev pump factor correction would calibrate the system flow rate output. As discussed in Section 4.1, the 0.2 gal/rev pump factor matches the manufacturer specifications.

4.1 Calibration Pre-Test

The flow rate into the system was calculated using the flow rate out of the system and the volume change per second inside of the 53 gallon velocity tank. The fluid area of the velocity tank was unknown since a bulkhead, the baffle system and the ultrasonic level sensor shielding PVC pipe occupied the tank volume. A volumetric pump test determines the fluid area of the velocity tank with the necessary equipment installed inside. In this test, the PCP pump runs at a fixed RPM with a prefilled velocity tank level of 10.125 in. The proximity sensor counts the number of pump rotor rotations per minute while displacing 10.125 in. of fluid from the velocity tank to define the tank area. Three tests produce an average 79.3 revolutions and a velocity tank area of 361.8 sq.in. The velocity tank area is found by multiplying the average number of rotations by 0.2 gal/rev pump factor, converting to cubic inches, and dividing the result by the 10.125 in. of displaced fluid height. The product of the change in fluid level velocity and the tank area identifies the rate of accumulation. The rate of accumulation can be added to the flow rate out, to calculate the volumetric return flow rate. The calculated volumetric return flow rate is important because it allows an accurate representation of the return flow rate the system is transient.

4.2 Single Fixed Volume Influx Simulation

Several tests evaluate how the flow rate system sensor responds to an immediate influx or burp of fluid entering the system. The test design involved evaluating a constant flow rate entering the velocity tank to simulate normal drilling operations and determine a baseline flow rate in gpm. Once established, a fixed amount of pre-measured fluid would enter the velocity tank over a 10.0 s period. The system flow rate should increase in RPM to mitigate the influx and remove it from the velocity tank before returning to the initial baseline flow rate.

4.2.1 Test #1 – Single Fixed Volume Influx

For the first test, the submersible pump and butterfly valve were used to create a constant flow rate of 18.0 ±1.2 gpm into the velocity tank. Within 10.0 s, 1.0 gal of water was added to the baffle system inside the velocity tank. See Figure 4.1 for the LabVIEW results of Test #1. See Table 4.2 below for a detailed summary of the test results compiled from Test #1.

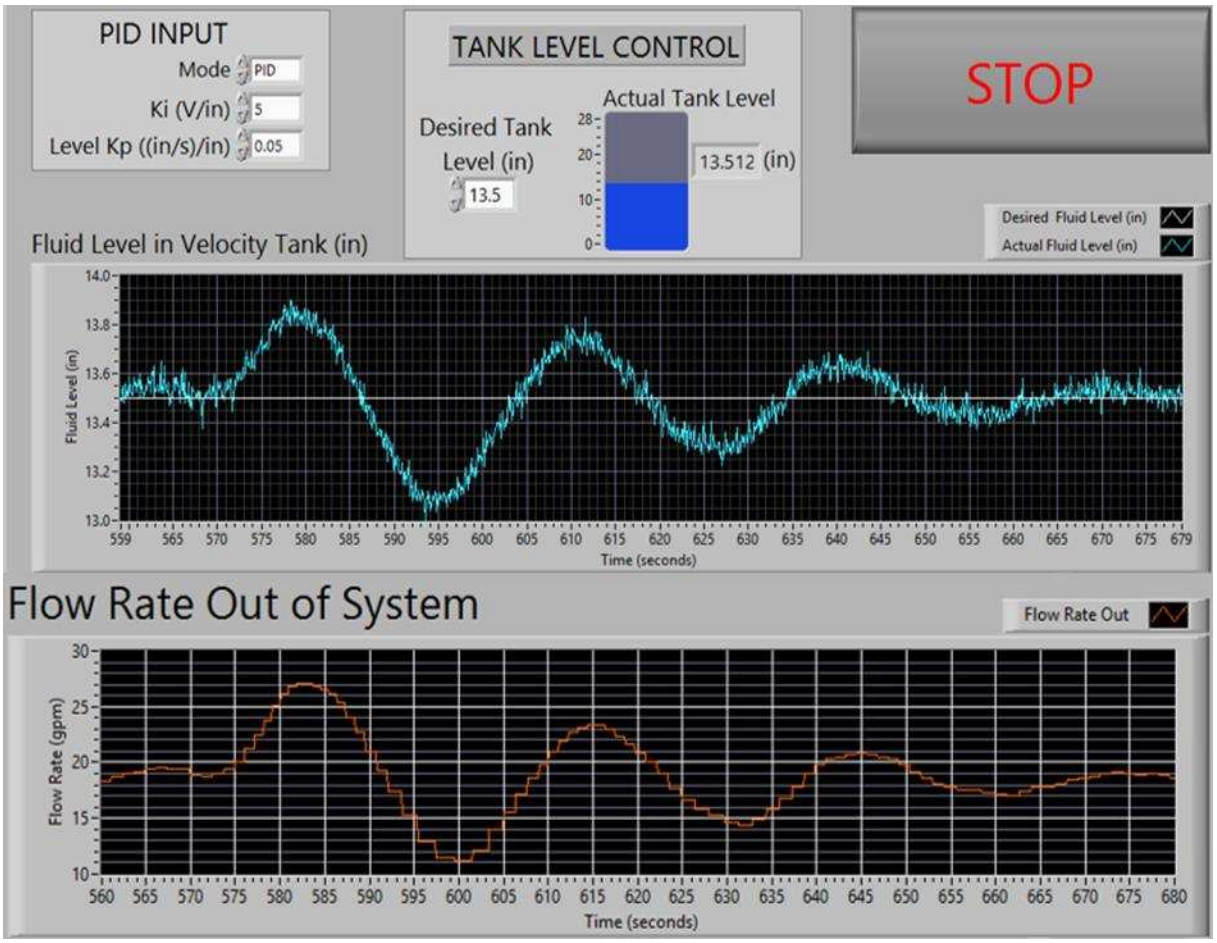

Figure 4.1 Test #1 fluid level and flow rate reaction in LabVIEW.

Table 4.2 Test #1: Summary of Results

Summary of Results: Test #1								
Initial System Parameters								
Initial Fluid Level (in.)	Initial Flow Rate (gpm)	Control System Settings		Ki (V/in.)	5.0			
13.5	18.0 ± 1.2			Level Kp ((in./s)in.)	0.05			
Test Design								
Test Type	Single Fixed Volume Influx - 1.0 gal							
Method Added	Gradually added with bucket							
Time Added	at 565.1 s over 10.0 s period							
Test Results								
Fluid Level Data Analysis								
Time Fluid Level Change Identified	568.6	s		Level Delay	3.5	s		
Max Mean Fluid Level	13.85	in.		Change	0.35	in.		
Time to Reach Steady-State Error	677.0	s		Overshoot	45.2	%		
Maximum Fluid Level Velocity	0.07	in./s		Settling Time	108.4	s		
Number of Overshoots	2				1.8	min		
Control System Settings Optimized?	No			Steady-State Error	0.67	%		
Flow Rate Data Analysis								
Initial Return Line Flow Rate	18.0	gpm		Control Deadtime	4.4	s		
Time Flow Rate Ramp Initiated	573.0	s		Total Delay	7.9	s		
Maximum Flow Rate Pumped	27.00	gpm		Change From Initial Flow Rate	50.0	%		
Final Return Line Flow Rate	18.60	gpm			3.3	%		
Expected Flow Rate Range	19.2	gpm		Theoretical Flow Rate	18.0	gpm		
	16.8	gpm		Flow Rate Accuracy	96.7	%		

The results from Test #1 indicate two different types of delay in the system as predicted by (Control Guru 2017; Lipták 1999). Figure 4.2 illustrates the initial delay as the time between fluid entering the baffle and the ultrasonic sensor detecting a change in fluid level. The second delay in the system is the control deadtime found in Table 4.2. Deadtime is the delay in pump response once a change in fluid level is identified. This is the system processing or computing time delay. The control deadtime for this system during Test #1 is 4.4 s.

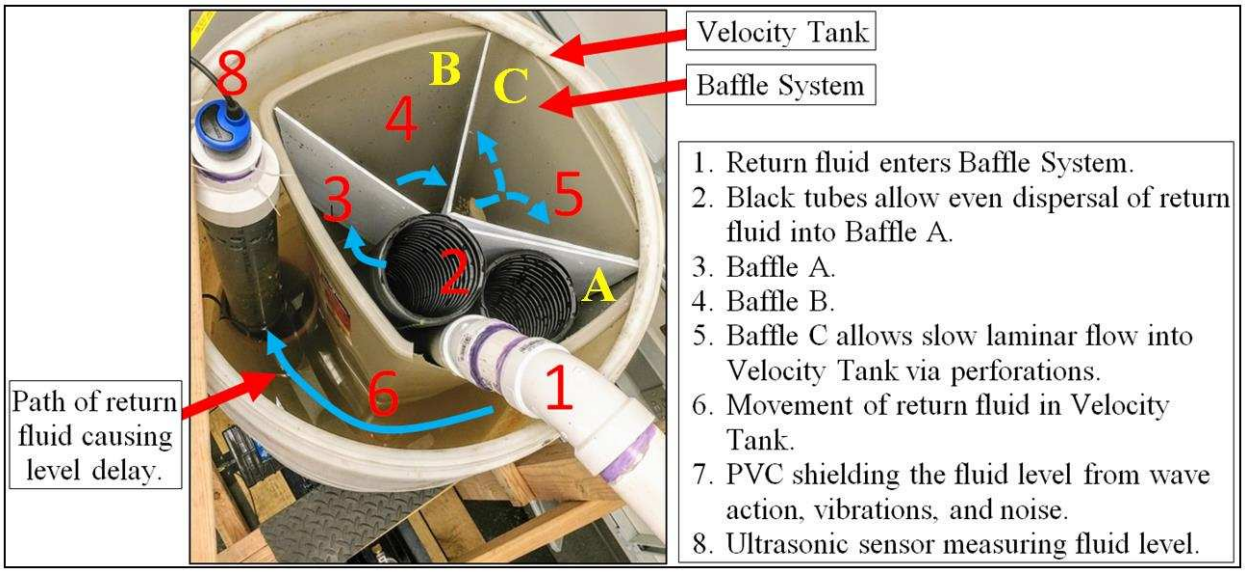

Figure 4.2 Flow path of return fluid through baffle system.

This means that the sum of these two delays (7.9 s) is the total delay in the system an influx enters, to the time right before the excess fluid is pumped out of the system. Also worth noting is the number of overshoots or oscillations in the fluid level as shown in Figure 4.1. The flow rate stabilized after 108.4 s of heavy oscillation. A high integral gain prompted integral windup that led to the heavy oscillation during the first test. The effect of integral windup is tuned by decreasing K_i and slightly decreasing the level proportional gain (K_p).

4.2.2 Test #2 – Single Fixed Volume Influx with Gain Change

Test #2 repeated the same procedure as Test #1 in that 1.0 gal was added to the baffles over a 10.0 s period, but the control system used an integral K_i setting of 4.5 V/in. instead of 5.0 V/in. The purpose of Test #2 is to demonstrate the behavior of the control system when reducing the integral gain by 0.5 V/in. See Figure 4.3 for the LabVIEW results of Test #2.

The settling time was 18.4 s shorter in Test #2 than in Test #1, indicating that a smaller integral controller reduced the time required to reach steady-state error. Observed in the results, the fluid level and flow stabilized after 90.0 s during oscillation due to integral windup. The amplitude of the oscillations was almost half of the amplitude recorded in Test #1; indicating that a smaller integral controller helped reduced the time required to reach steady-state error sooner. Assuming this trend remains true for this system; a lower K_i and K_p should practically eliminate integral windup and prevent or reduce overshoot. See Table 4.3 for a detailed summary of the

test results compiled from Test #2.

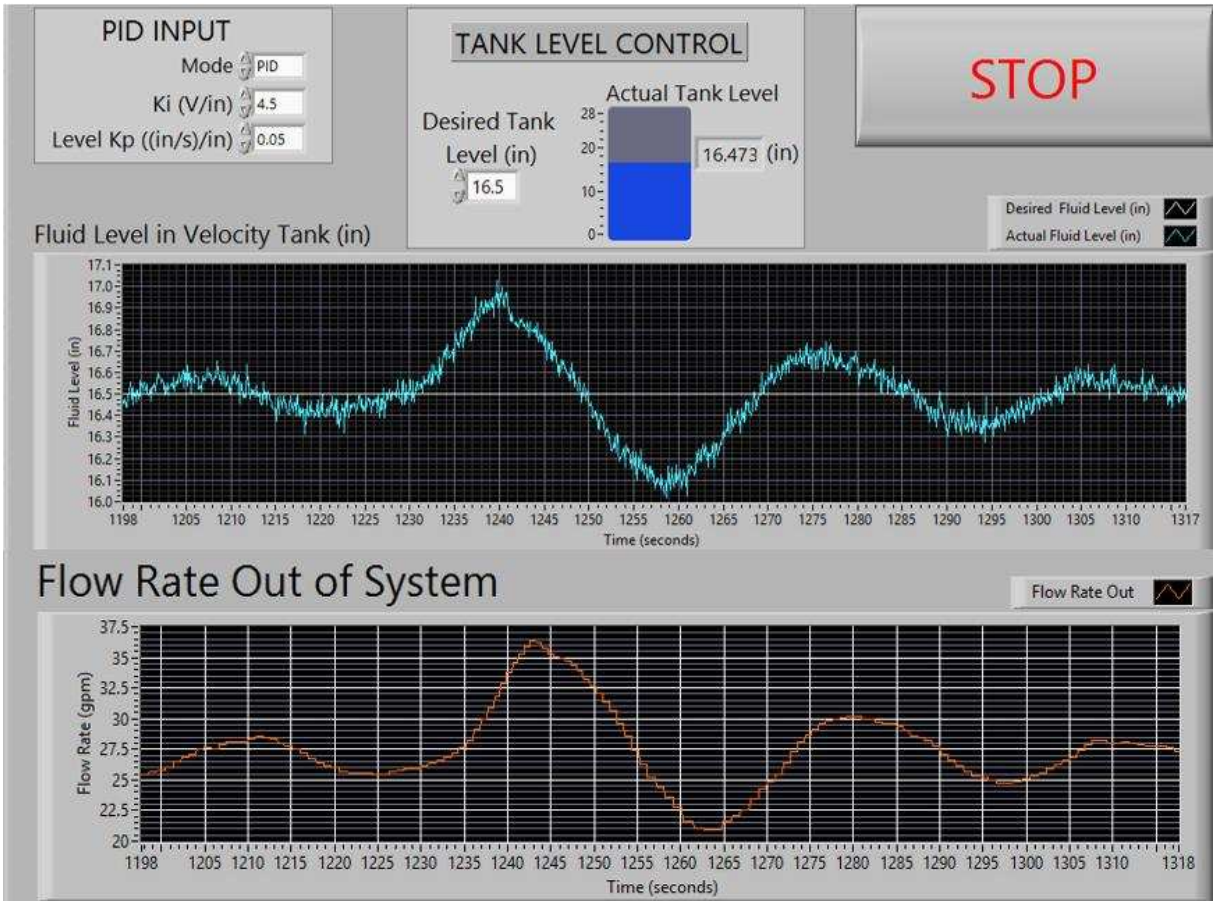

Figure 4.3 Test #2 fluid level and flow rate reaction in LabVIEW.

The results in Table 4.3 indicate a longer level delay (9.8 s) compared to the 3.5 s in Test #1. Since the test was executed in the same manner, it is unexpected that an additional 6.3 s delay prolonged ultrasonic sensor from identifying a change in fluid level. The most logical explanation is that the residual integral windup leading to the fluid level decreasing the moment before the gallon influx was added the baffles. The drop in fluid level extended from time 1212.0 s to 1229.0 s and possessed a negative amplitude of 0.09 in. Since the 1.0 gallon influx was added at time 1215.2 s, the ultrasonic level sensor would not have been able to measure an influx above the target level because the fluid level was already decreasing at that time. This clarifies the prolonged level delay observed in Test #2 and identified the importance of addressing integral windup before testing to reduce inaccuracy of results.

Table 4.3 Test #2: Summary of Results

Summary of Results: Test #2							
Initial System Parameters							
Initial Fluid Level (in.)	Initial Flow Rate (gpm)	Control System Settings		Ki (V/in.)	4.5		
16.5	27.0 ± 1.5			Level Kp ((in./s)in.)	0.05		
Test Design							
Test Type	Single Fixed Volume Influx - 1.0 gal						
Method Added	Gradually added with bucket						
Time Added	at 1215.2 s over 10.0 s period						
Test Results							
Fluid Level Data Analysis							
Time Fluid Level Change Identified	1225.0	s		Level Delay	9.8	s	
Max Mean Fluid Level	16.95	in.		Change	0.45	in.	
Time to Reach Steady-State Error	1315.0	s		Overshoot	33.2	%	
Maximum Fluid Level Velocity	0.07	in./s		Settling Time	90.0	s	
Number of Overshoots	2				1.5	min	
Control System Settings Optimized?	No			Steady-State Error	0.61	%	
Flow Rate Data Analysis							
Initial Return Line Flow Rate	27.0	gpm		Control Deadtime	2.6	s	
Time Flow Rate Ramp Initiated	1227.6	s		Total Delay	12.4	s	
Maximum Flow Rate Pumped	36.50	gpm		Change From Initial	35.2	%	
Final Return Line Flow Rate	27.40	gpm		Flow Rate	1.5	%	
Expected Flow Rate Range	29.5	gpm		Theoretical Flow Rate	27.0	gpm	
	26.5	gpm		Flow Rate Accuracy	98.5	%	

4.2.3 Test #3 – Small Single Fixed Volume Influx

Integral K_i and Level K_p gains were tuned to eliminate integral windup and excessive oscillation. The K_i control was set to 3.0 V/in. and the Level K_p gain was set to 0.02 (in./s)/in. The submersible pump and butterfly valve were used to create a constant flow rate of 6.0 ±0.2 gpm. At time 850.5 s, 0.5 gal of water was added to the velocity tank within 10.0 s. See Figure 4.4 for the LabVIEW results of Test #3.

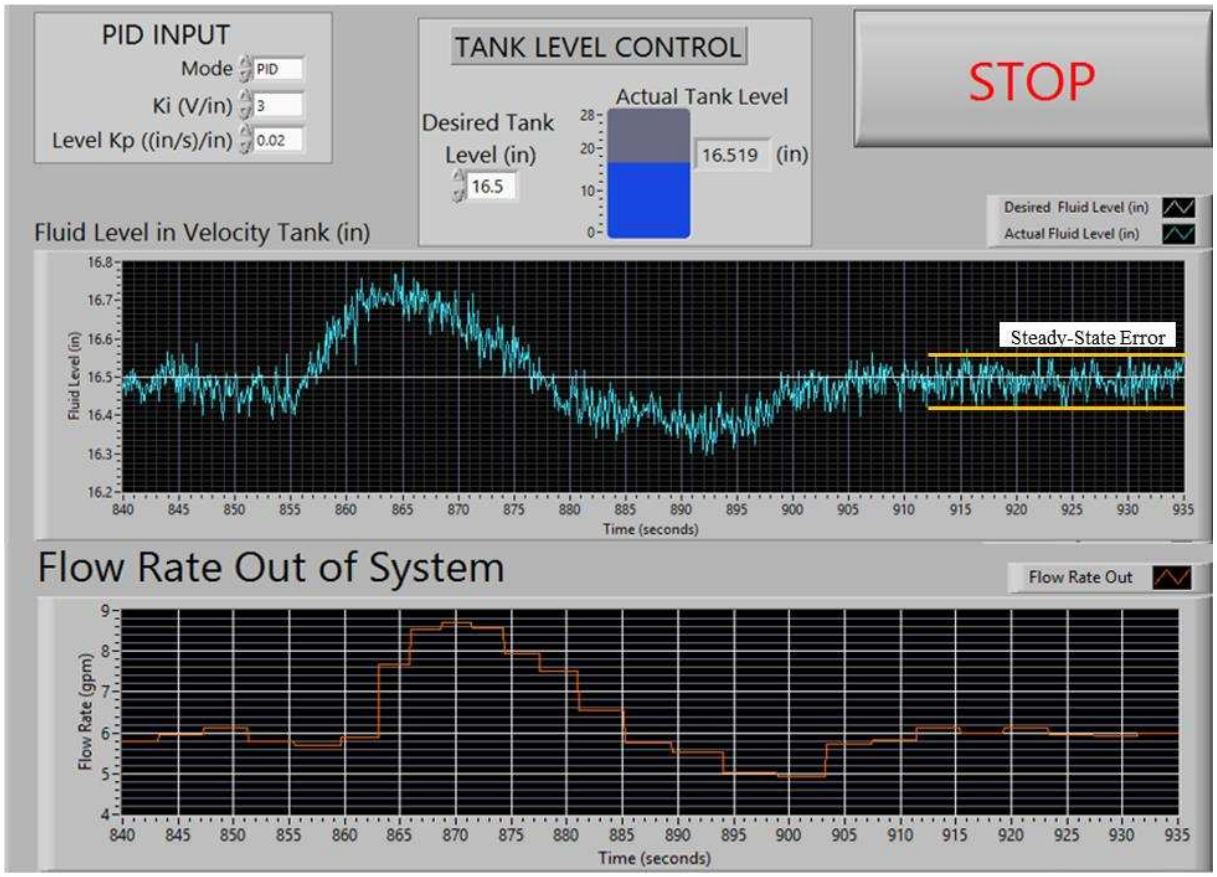

Figure 4.4 Test #3 fluid level and flow rate reaction in LabVIEW.

After mitigating the influx, the final flow rate returned to the exact initial 6.0 gpm flow rate and reached the settling time within 50.5 s. This system produced a lower settling time than Test #1 and Test #2 but is still not a balanced system due to overshoot. The settling time was reached 57.9 s sooner than Test #1 and 39.5 s sooner than Test #2. See Table 4.4 for a detailed summary of the test results compiled from Test #3.

The results in Table 4.4 indicate another increase in level delay. Figure 4.4, shows fluid level decreasing between time 845.0 s and 855.0 s. Similar to Test #2, the fluid level in Test #3 decreases below the desired tank level and a 0.5 gal influx is added to the system (850.5 s). This results in a level delay of 6.0 s and a control deadtime of 6.5 s. The total system response delay is 12.5 s, meaning that once the influx enters the system, there is no change in PCP RPM for over 12.0 s. Therefore, it takes the Active Control VFR Meter more time to change the pump RPM when an influx enters the velocity tank and the fluid level is decreasing below the target level. It is likely that this requires a deeper investigation outside of the current scope of research to

identify a method to cope with this cyclic fluid level within the steady-state error.

Table 4.4 Test #3: Summary of Results

Summary of Results: Test #3								
Initial System Parameters								
Initial Fluid Level (in.)	Initial Flow Rate (gpm)	Control System Settings			Ki (V/in.)	3.0		
16.5	6.0 ± 0.2				Level Kp ((in./s)in.)	0.02		
Test Design								
Test Type	Single Fixed Volume Influx - 0.5 gal							
Method Added	Gradually added with bucket							
Time Added	at 850.5 s over 10.0 s period							
Test Results								
Fluid Level Data Analysis								
Time Fluid Level Change Identified	856.5	s			Level Delay	6.0	s	
Max Mean Fluid Level	16.7	in.			Change	0.20	in.	
Time to Reach Steady-State Error	907.0	s			Overshoot	45.0	%	
Maximum Fluid Level Velocity	0.06	in./s			Settling Time	50.5	s	
Number of Overshoots	1					0.8	min	
Control System Settings	No				Steady-State Error	0.30	%	
Flow Rate Data Analysis								
Initial Return Line Flow Rate	6.0	gpm			Control Deadtime	6.5	s	
Time Flow Rate Ramp Initiated	863.0	s			Total Delay	12.5	s	
Maximum Flow Rate Pumped	8.70	gpm			Change From Initial	45.0	%	
Final Return Line Flow Rate	6.00	gpm			Flow Rate	0.0	%	
Expected Flow Rate Range	6.7	gpm			Theoretical Flow Rate	6.0	gpm	
	6.3	gpm			Flow Rate Accuracy	100.0	%	

4.3 Fixed Flow Rate Influx Simulation

Several tests were designed to evaluate how the flow rate system sensor responds to a continuous influx of fluid added to the system's existing flow rate. The design of the test needed to simulate normal drilling operations. When tested, the system would determine a baseline flow rate in gpm. Once established, a fixed flow rate resembling an influx would enter the velocity

tank for the duration of the test. The PCP should increase in RPM to mitigate the influx, match the flow rate, and remove fluid volume above the initial desired fluid level. The system should then maintain the fluid level at the predetermined level and match the new total system flow rate including the influx flow rate.

4.3.1 Test #4 - Fixed Flow Rate Influx

A constant flow rate of 6.0 ±0.4 gpm was supplied using the submersible pump and butterfly valve. An influx with a fixed rate of 4.4 gpm was added to the velocity tank at time 555.1 s. See Figure 4.5 for the LabVIEW results of Test #4.

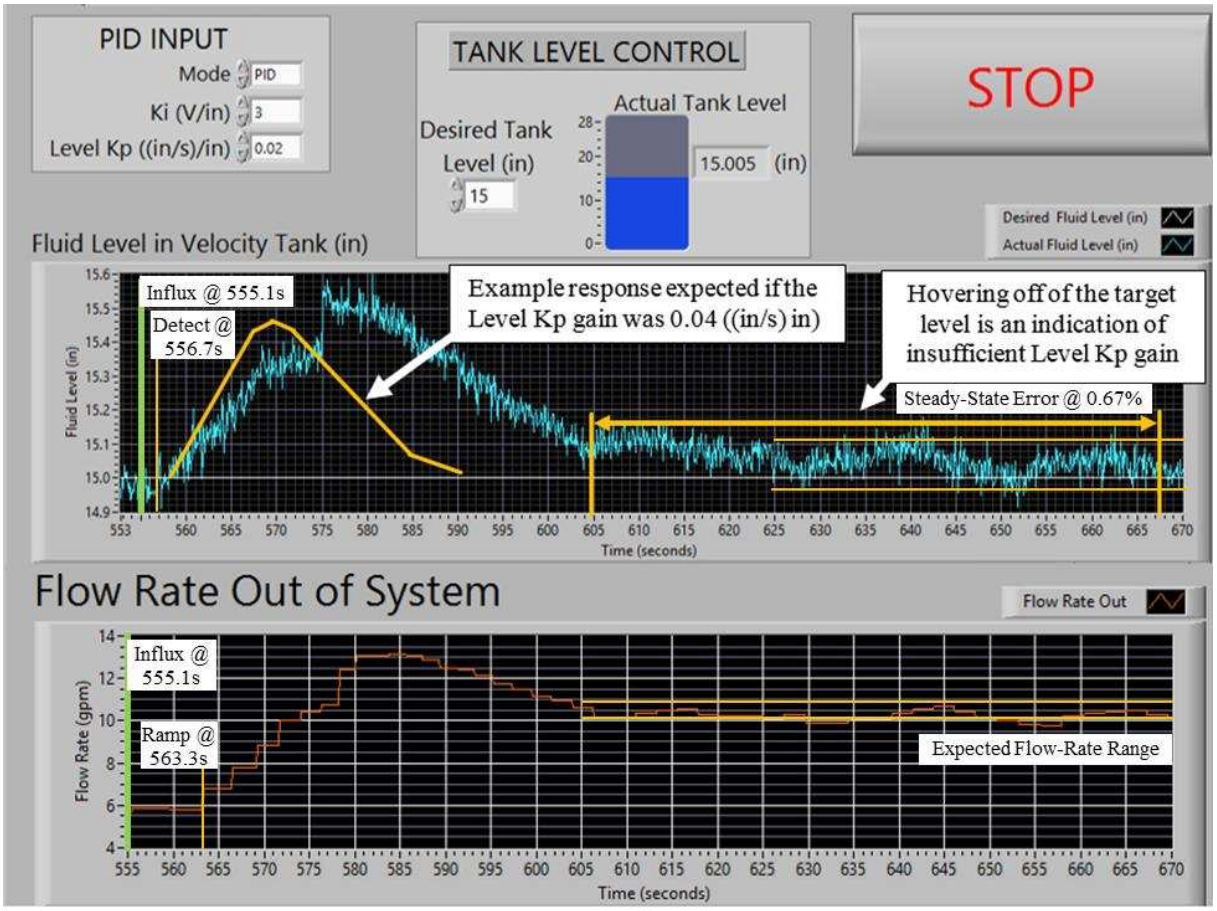

Figure 4.5 Test #4 fluid level and flow rate reaction in LabVIEW.

The flow rate out for Test #4 increased to 13.3 gpm to mitigate the extra fluid level above the set point of 15.0 in. The controller and pump brought the fluid level back to 15.0 in. within 68.3 s after the ultrasonic sensor detected a fluid influx. The final return flow rate is 10.2 gpm and falls within the expected range 10.0 gpm and 10.8 gpm. Control Guru (2017) explains why

the system responded quickly to identify, control, mitigate, and match the flow rate entering the system. See Table 4.5 for a detailed summary of the test results compiled from Test #4.

Table 4.5 Test #4: Summary of Results

Summary of Results: Test #4							
Initial System Parameters							
Initial Fluid Level (in.)	Initial Flow Rate (gpm)	Control System Settings		Ki (V/in.)	3.0		
15.0	6.0 ± 0.4			Level Kp ((in./s)in.)	0.02		
Test Design							
Test Type	Fixed Flow Rate Influx of 4.4 gpm						
Method Added	Fixed pressure hose from sink (cold) immediate increase						
Time Added	at 555.1 s for the remainder of the test						
Test Results							
Fluid Level Data Analysis							
Time Fluid Level Change Identified	557	s		Level Delay	1.6	s	
Max Mean Fluid Level	15.6	in.		Change	0.60	in.	
Time to Reach Steady-State Error	625.0	s		Overshoot	30.4	%	
Maximum Fluid Level Velocity	0.11	in./s		Settling Time	68.3	s	
Number of Overshoots	0				1.1	min	
Control System Settings Optimized?	Yes			Steady-State Error	0.67	%	
Flow Rate Data Analysis							
Initial Return Line Flow Rate	5.9	gpm		Control Deadtime	6.6	s	
Time Flow Rate Ramp Initiated	563.3	s		Total Delay	8.2	s	
Maximum Flow Rate Pumped	13.30	gpm		Change From Initial	125.4	%	
Final Return Line Flow Rate	10.20	gpm		Flow Rate	72.9	%	
Expected Flow Rate Range	10.8	gpm		Theoretical Flow Rate	10.4	gpm	
	10.0	gpm		Flow Rate Accuracy	98.1	%	

Unlike the first three tests, the results in Table 4.4 indicated a very small level delay (1.6 s). The delay is lower in this test because of the high volume of fluid entering the velocity tank combined with the pressure fed flow rate influx. When the fluid entering the velocity tank is under pressure, fluid will force its way to the opposite side of the tank faster than gravity could rearrange the same volume. Therefore, the increase in fluid level is almost instantaneous as pressure increases with an increase in fluid height. With a 4.4 gpm influx, the fluid height inside

of the baffle would increases rapidly (about the ultrasonic sensor sensitivity of 0.125 in.) in a short period until the PCP flow rate increases. Evidence suggests that a more aggressive K_p could have mitigated target hover and may have resulted in a lower settling time.

4.3.2 Test #5 - Fixed Flow Rate Influx

A constant flow rate of 6.0 ±0.2 gpm was supplied using the submersible pump and butterfly valve. An influx with a steady flow rate of 5.9 gpm was added to the velocity tank at time 195.0 s. See Figure 4.6 for the LabVIEW results of Test #5.

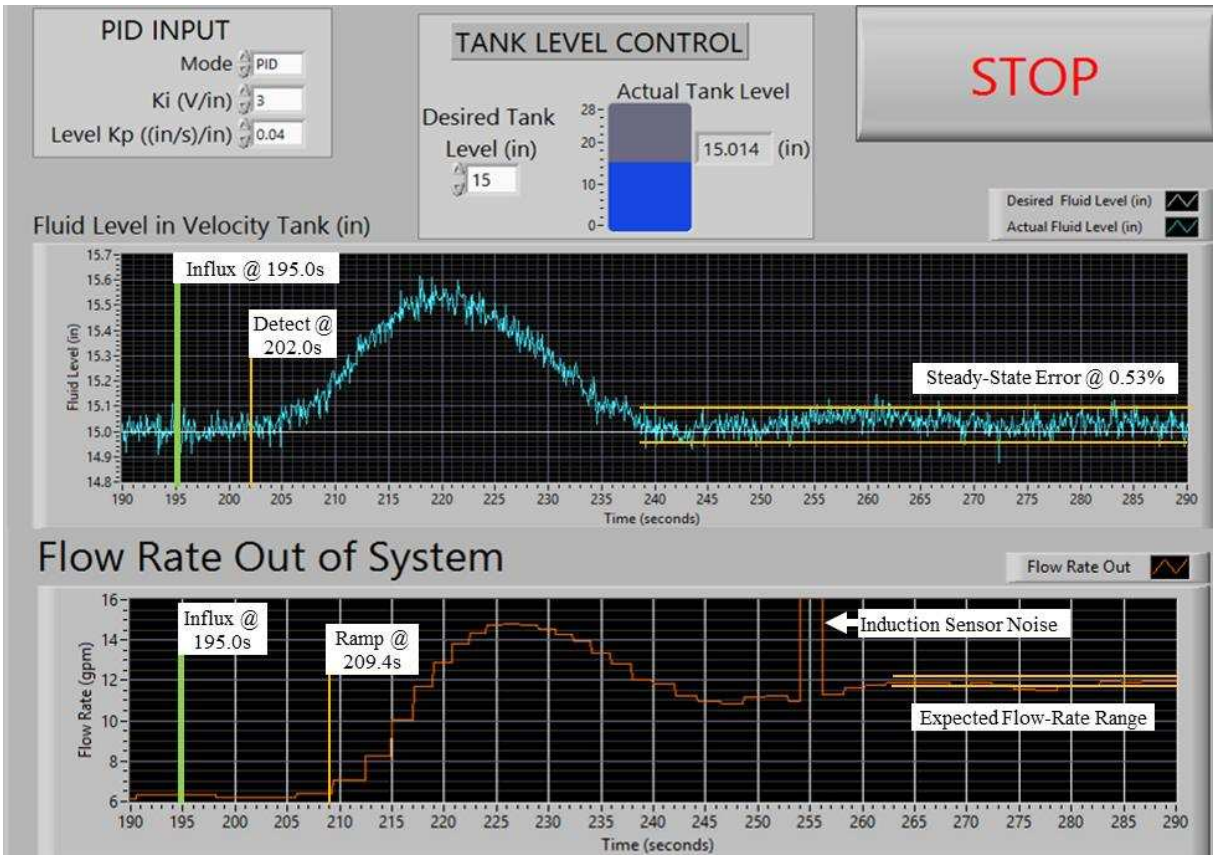

Figure 4.6 Test #5 fluid level and flow rate reaction in LabVIEW.

The PCP flow rate increased from 6.0 ±0.2 gpm to 14.7 gpm to mitigate the extra fluid level above the initial desired fluid level of 15.0 in. The controller rapidly ramped up the PCP flow rate to quickly return the fluid level back to 15.0 in. Once the ultrasonic sensor detected a fluid influx in the system, it only took 38.0 s to bring the fluid level back to the set point and match the combined system flow rates. Since the initial flow rate of the system was 6.0 ±0.2 gpm and the influx flow rate was 5.9 gpm, the expected total flow rate should fall between 11.7 gpm

and 12.1 gpm. As indicated in Figure 4.6, the final flow rate determined was 11.98 gpm. See Table 4.6 for a detailed summary of the test results compiled from Test #5.

Table 4.6 Test #5: Summary of Results

Summary of Results: Test #5								
Initial System Parameters								
Initial Fluid Level (in.)	Initial Flow Rate (gpm)	Control System Settings		Ki (V/in.)	3.0			
15.0	6.0 ± 0.2			Level Kp ((in./s)in.)	0.04			
Test Design								
Test Type	Fixed Flow Rate Influx of 5.9 gpm							
Method Added	Fixed pressure hose from sink (hot & cold) immediate increase							
Time Added	at 195.0 s for the remainder of the test							
Test Results								
Fluid Level Data Analysis								
Time Fluid Level Change Identified	202.0	s		Level Delay	7.0	s		
Max Mean Fluid Level	15.54	in.		Change	0.54	in.		
Time to Reach Steady-State Error	240.0	s		Overshoot	22.7	%		
Maximum Fluid Level Velocity	0.06	in./s		Settling Time	38.0	s		
Number of Overshoots	0				0.6	min		
Control System Settings Optimized?	Yes			Steady-State Error	0.53	%		
Flow Rate Data Analysis								
Initial Return Line Flow Rate	6.0	gpm		Control Deadtime	7.4	s		
Time Flow Rate Ramp Initiated	209.4	s		Total Delay	14.4	s		
Maximum Flow Rate Pumped	14.70	gpm		Change From Initial Flow Rate	145.0	%		
Final Return Line Flow Rate	11.98	gpm			99.7	%		
Expected Flow Rate Range	12.1	gpm		Theoretical Flow Rate	11.9	gpm		
	11.7	gpm		Flow Rate Accuracy	99.3	%		

The difference in controller performance observed in Test #4 and Test #5 was significant since the only difference between the controls settings used was the 0.04 Level K_p used in Test #5 versus the 0.02 Level K_p used in Test #4. When comparing the settling time and the number of overshoots, the controller settings used in Test #5 outperformed all other tests. The controller settings were optimally tuned for the specific scenario presented in Test #5, but it is unlikely that

the manually set gains would work as well in different flow rate scenarios or loss circulation events. The implementation of an advanced autotuning PID controller could result in exceptional controller performance in different scenarios without having to tune the controller manually.

4.3.3 Test #6 – Multiple Fixed Flow Rate Influxes

A constant flow rate of 5.8 ±0.3 gpm was created using the submersible pump and butterfly valve. Two different influx flow rates were added to the initial flow rate at two separate points in time. At time 580.0 s, an increase in flow rate was made with the butterfly valve by moving the locking butterfly valve position from the initial #5 position to the #6 position for a 9.4 gpm increase. Additionally, a continuous influx of 4.4 gpm was added to the system at time 615.0 s. See Figure 4.7 for the LabVIEW results of Test #6.

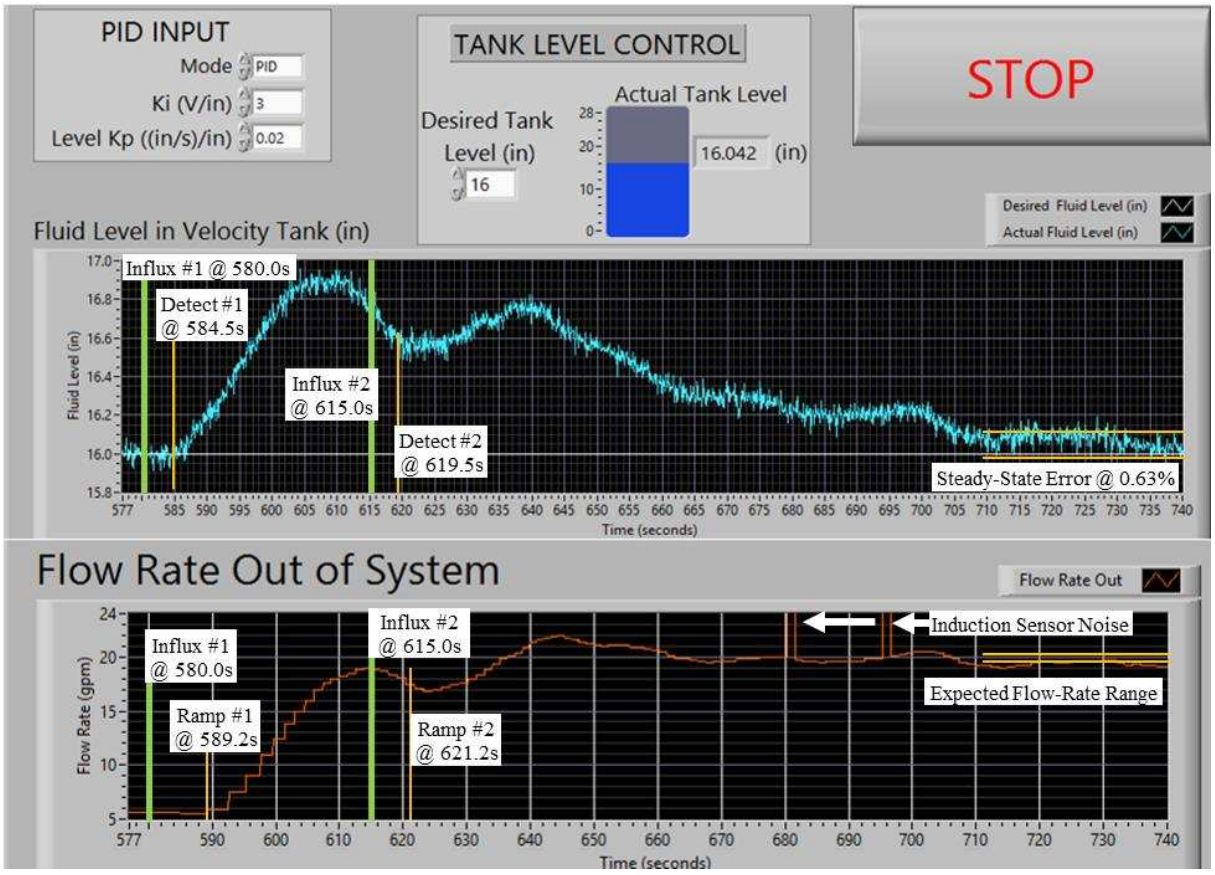

Figure 4.7 Test #6 fluid level and flow rate reaction in LabVIEW.

Flow rates for Test #6 increased from the initial 5.8 ±0.3 gpm to roughly 19.0 gpm at time 614.0 s. A fixed flow rate 4.4 gpm influx entered the system at 615.0 s. The final flow rate of the system should fall between 19.3 gpm and 19.9 gpm. As indicated in Figure 4.7, the final average

flow rate determined was roughly 19.3 gpm. See Table 4.7 for a detailed summary of the results compiled from Test #6.

Table 4.7 Test #6: Summary of Results

Summary of Results: Test #6								
Initial System Parameters								
Initial Fluid Level (in.)	Initial Flow Rate (gpm)	Control System Settings		Ki (V/in.)	3.0			
16.0	5.8 ± 0.3			Level Kp ((in./s)in.)	0.02			
Test Design								
Test Type	Multiple Fixed Flow Rate Increases of 9.4 & 4.4 gpm							
Method Added	Butterfly moved from #5 position to #6 position and							
	Fixed pressure hose from sink (cold) immediate increase							
Time Added	at 580.0 s for the remainder of the test							
	at 615.0 s for the remainder of the test							
Test Results								
Fluid Level Data Analysis								
Fluid Level Change #1 Identified	584.5	s		Level Delay #1	4.5	s		
Fluid Level Change #2 Identified	619.5	s		Level Delay #2	4.5	s		
Max Mean Fluid Level	16.9	in.		Change	0.90	in.		
Time to Reach Steady-State Error	730.0	s		Influx 2 Overshoot	14.0	%		
Maximum Fluid Level Velocity	0.07	in./s		Steady-State Error	0.63	%		
Number of Overshoots	0			Settling Time	115.0	s		
Control System Settings Optimized?	Yes				1.9	min		
Flow Rate Data Analysis								
Initial Return Line Flow Rate	5.8	gpm		Control Deadtime #1	4.7	s		
Time Flow Rate Ramp 1 Initiated	589.2	s		Control Deadtime #2	1.7	s		
Time Flow Rate Ramp 2 Initiated	621.2	s		Total Delay	9.2	s		
Maximum Flow Rate Pumped	22.00	gpm						
Final Return Line Flow Rate	19.30	gpm		Change From Initial	279.3	%		
				Flow Rate	232.8	%		
Expected Flow Rate Range	19.9	gpm		Theoretical Flow Rate	19.6	gpm		
	19.3	gpm		Flow Rate Accuracy	98.5	%		

While it is impossible to identify the true settling time in this dynamic system, the estimated settling time for the second influx (115 s) could have been reduced with an increase in K_p. The percent increase in flow rate compared to the initial flow rate required a higher

proportional gain setting. An autotuning controller could have changed gains on the fly, returned to steady-state error, and identified the return VFR equal to the VFR out in a shorter time.

4.3.4 Test #7 - Fixed Flow Rate

A constant flow rate of 24.8 ±0.4 gpm was supplied using the submersible pump and butterfly valve. An influx with a constant flow rate of 0.8 gpm was added to the velocity tank at time 2205.0 s. See Figure 4.8 for the LabVIEW results of Test #7.

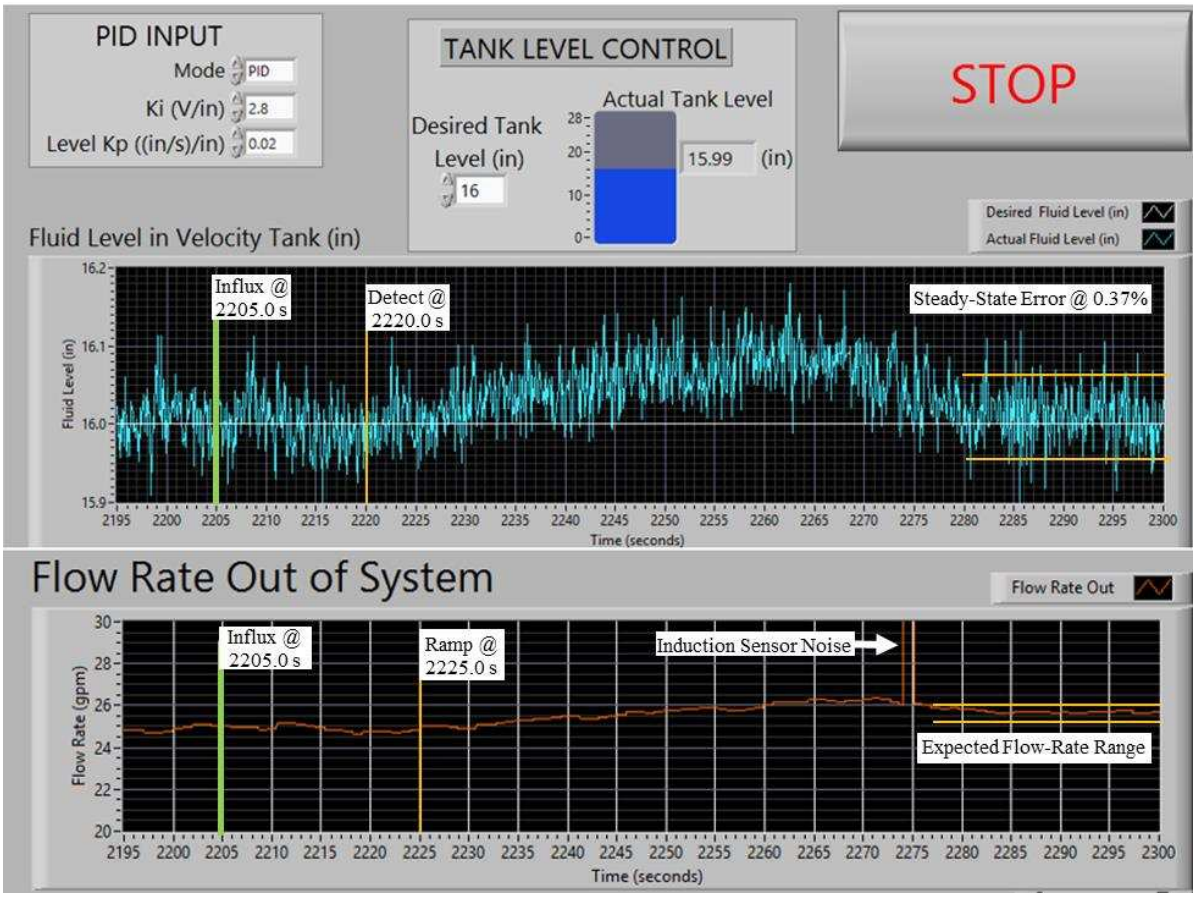

Figure 4.8 Test #7 fluid level and flow rate reaction in LabVIEW.

The flow rate increases after time 2225.0 s to a peak of 26.45 gpm to remove excess fluid from the velocity tank and return the fluid level to the target level at 16.0 in. The normal total flow rate of the system should fall between 25.2 gpm and 26.0 gpm. As indicated in Figure 4.8, the final average flow rate found was roughly 25.67 gpm and falls within the flow rate expected. The level delay was much longer than previous tests due to the very low flow rate (0.8 gpm). The system simply took longer to recognize the such a small influx. See Table 4.8 for a detailed summary of the results compiled from Test #7.

Table 4.8 Test #7: Summary of Results

Summary of Results: Test #7								
Initial System Parameters								
Initial Fluid Level (in.)	Initial Flow Rate (gpm)	Control System Settings		Ki (V/in.)	2.8			
16.0	24.8 ± 0.4			Level Kp ((in./s)in.)	0.02			
Test Design								
Test Type	Fixed Flow Rate Influx - 0.8 gpm							
Method Added	Fixed pressure hose from sink (cold) immediate increase							
Time Added	at 2205.0 s for the remainder of the test							
Test Results								
Fluid Level Data Analysis								
Time Fluid Level Change Identified	2220.0	s		Level Delay	15.0	s		
Max Mean Fluid Level	16.09	in.		Change	0.09	in.		
Time to Reach Steady-State Error	2285.0	s		Overshoot	3.0	%		
Maximum Fluid Level Velocity	0.07	in./s		Settling Time	65.0	s		
Number of Overshoots	0				1.1	min		
Control System Settings Optimized?	Yes			Steady-State Error	0.37	%		
Flow Rate Data Analysis								
Initial Return Line Flow Rate	24.75	gpm		Control Deadtime	5.0	s		
Time Flow Rate Ramp Initiated	2225.0	s		Total Delay	20.0	s		
Maximum Flow Rate Pumped	26.45	gpm		Change From Initial Flow Rate	6.9	%		
Final Return Line Flow Rate	25.67	gpm			3.6	%		
Expected Flow Rate Range	26.0	gpm		Theoretical Flow Rate	25.6	gpm		
	25.2	gpm		Flow Rate Accuracy	99.5	%		

4.4 Flow Rate Decrease/Loss Circulation Test Simulation

It is important for the system to have the capability to detect a fluid loss or decrease in flow rate within the system to warn of a possible loss circulation event. The design of the test needed to simulate normal drilling operations. When tested, the system would determine a baseline flow rate in gallons per minute. Once established, a fixed flow rate would be removed from the system to create a partial loss of fluid. The system should then allow the flow entering the velocity tank to fill the fluid void below the target level. The control system and PCP found the new flow rate at the end of the test.

4.4.1 Test #8 – Flow Rate Decrease

The pump, butterfly valve (#8 position), and 4.4 gpm hose were used to create a constant flow rate of 36.6 ±0.4 gpm. At time 865.0 s the total flow rate was decreased by 4.4 gpm. See Figure 4.9 for the LabVIEW results of Test #8.

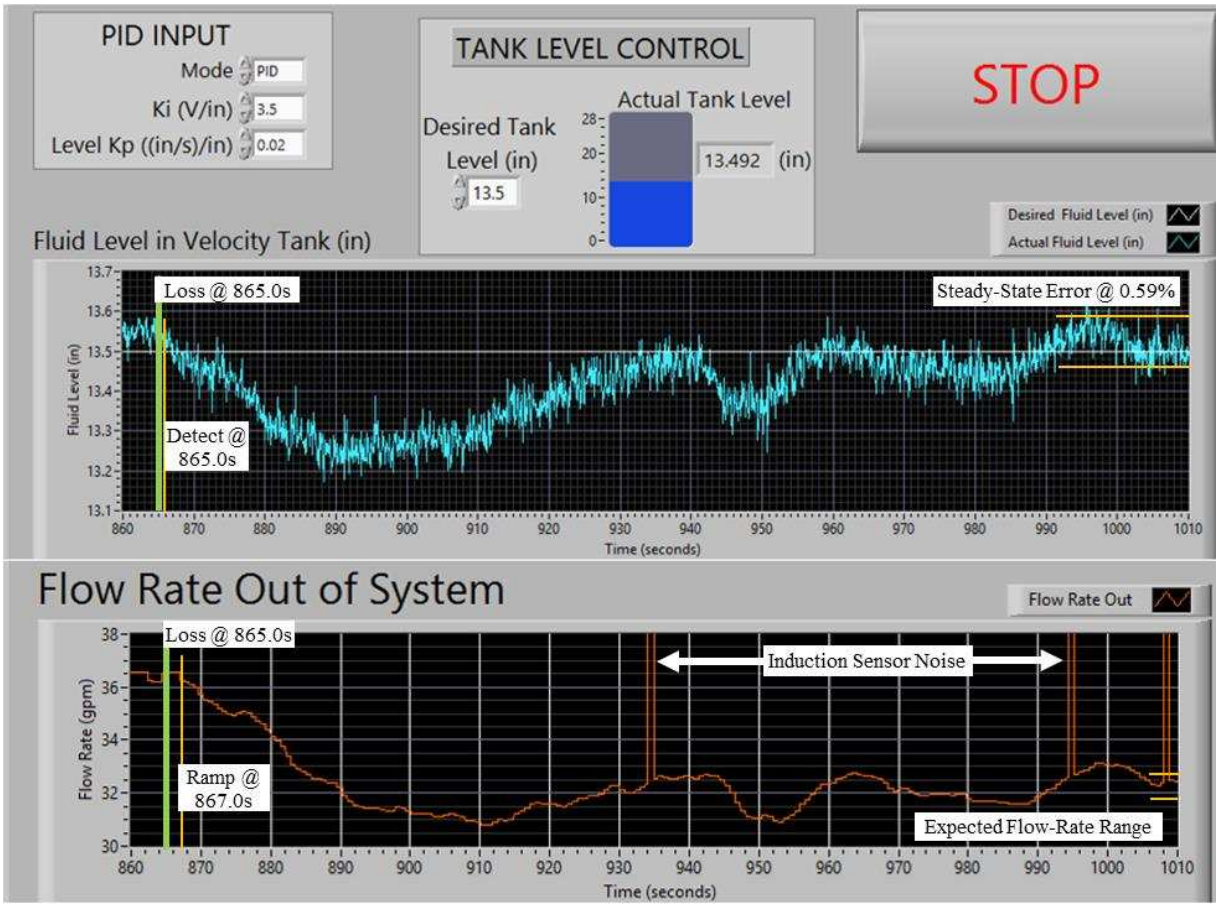

Figure 4.9 Test #8 fluid level and flow rate reaction in LabVIEW.

The fluid level dropped within 0.0 s when 4.4 gpm of flow was removed from the system. The flow rate determined in LabVIEW decreased from 36.6 gpm to the minimum flow rate of 30.7 gpm until the flow rate entering the velocity tank could increase the fluid level. The expected flow rate after removing the 4.4 gpm flow rate from the initial 36.5 gpm should fall between 31.8 gpm and 32.6 gpm. The final average flow rate determined was 32.4 gpm and falls within the expected range. See Table 4.9 for a detailed summary of the results compiled from Test #8.

Table 4.9 Test #8: Summary of Results

Summary of Results: Test #8							
Initial System Parameters							
Initial Fluid Level (in.)	Initial Flow Rate (gpm)	Control System Settings		Ki (V/in.)	3.5		
13.5	36.6 ± 0.4			Level Kp ((in./s)in.)	0.02		
Test Design							
Test Type	Fixed Flow Rate loss of 4.4 gpm						
Method Added	Fixed pressure hose from sink (cold) immediate shut off						
Time Removed	at 865.0 s for the remainder of the test						
Test Results							
Fluid Level Data Analysis							
Time Fluid Level Change Identified	865.0	s		Level Delay	0.0	s	
Minimum Mean Fluid Level	13.2	in.		Change	-0.26	in.	
Time to Reach Steady-State Error	990.1	s		Overshoot	-5.2	%	
Minimum Fluid Level Velocity	-0.04	in./s		Settling Time	125.1	s	
Number of Overshoots	2				2.1	min	
Control System Settings Optimized?	No			Steady-State Error	0.59	%	
Flow Rate Data Analysis							
Initial Return Line Flow Rate	36.55	gpm		Control Deadtime	2.0	s	
Time Flow Rate Ramp Initiated	867.0	s		Total Delay	2.0	s	
Minimum Flow Rate Pumped	30.70	gpm		Change From Initial	-16.0	%	
Final Return Line Flow Rate	32.40	gpm		Flow Rate	-12.8	%	
Expected Flow Rate Range	32.6	gpm		Theoretical Flow Rate	32.2	gpm	
	31.8	gpm		Flow Rate Accuracy	99.2	%	

4.4.2 Test #13 – Flow Rate Decrease

The pump, butterfly valve (#6 position), and 4.4 gpm hose were used to create a constant flow rate of 20.8 ±0.6 gpm. At time 540.0 s the total flow rate was decreased by 4.4 gpm. See Figure 4.10 for the LabVIEW results of Test #13. The level delay was 4.3 s after 4.4 gpm of flow was removed from the system. The flow rate determined in LabVIEW decreased from 20.8 gpm to the minimum flow rate of 13.9 gpm until the flow rate entering the velocity tank could increase the fluid level. The expected flow rate after removing the 4.4 gpm flow rate from the

initial 20.8 gpm should fall between 15.8 gpm and 17.0 gpm. The final average flow rate determined was 16.8 gpm and falls within the expected range. See Table 4.10 for a detailed summary of the results compiled from Test #13.

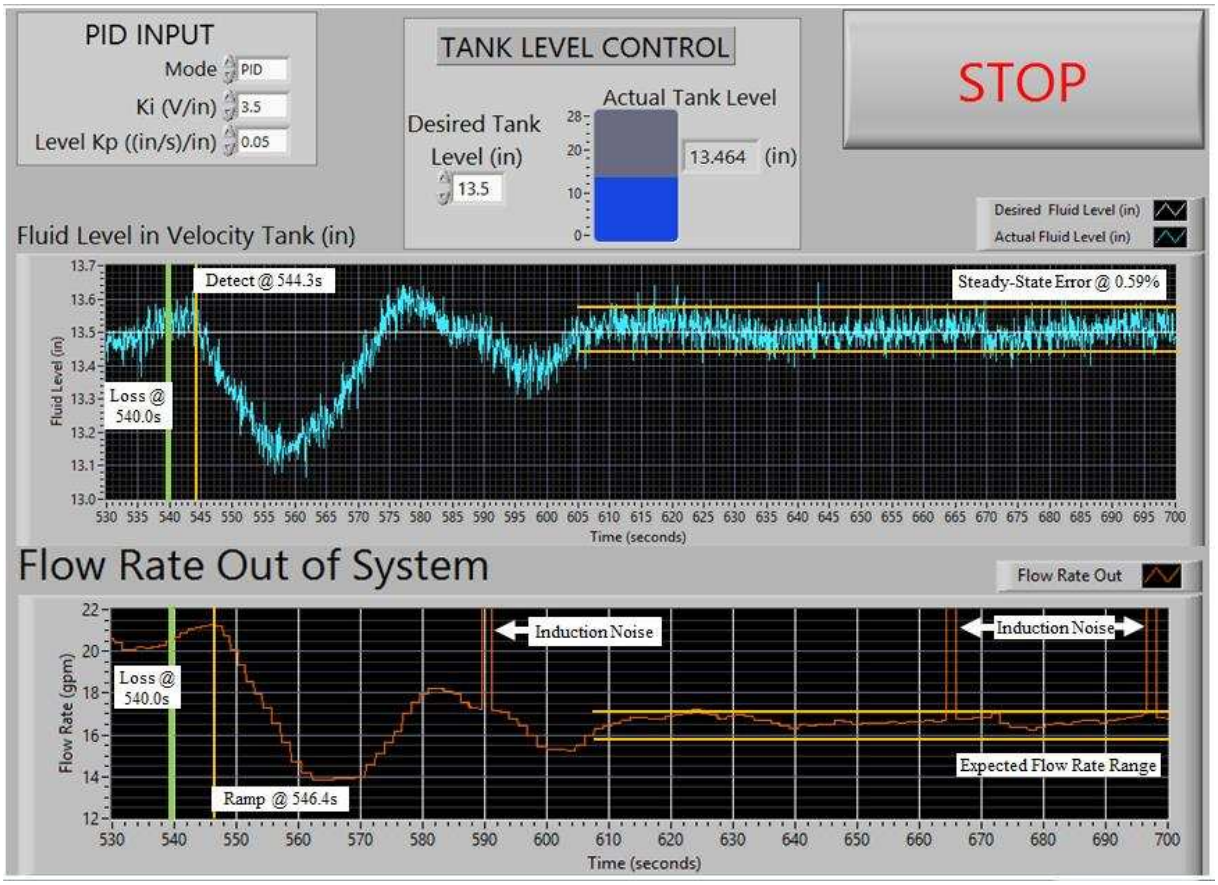

Figure 4.10 Test #13 fluid level and flow rate reaction in LabVIEW.

The results identified from Test #13 identify that controller system settings were not optimized since the controller overshot the target level, resulting in a settling time of 60.7 s. The flow rate accuracy for Test #13 is 97.6%.

Table 4.10 Test #13: Summary of Results

Summary of Results: Test #13							
Initial System Parameters							
Initial Fluid Level (in.)	Initial Flow Rate (gpm)	Control System Settings		Ki (V/in.)	3.5		
13.5	20.8 ± 0.6			Level Kp ((in./s)in.)	0.05		
Test Design							
Test Type	Fixed Flow Rate loss of -4.4 gpm						
Method Removed	Fixed pressure hose from sink (cold) immediate shut off						
Time Removed	at 540.0 s for the remainder of the test						
Test Results							
Fluid Level Data Analysis							
Time Fluid Level Change Identified	543.5	s		Level Delay	3.5	s	
Min Mean Fluid Level	13.1	in.		Change	-0.36	in.	
Time to Reach Steady-State Error	605.0	s		Overshoot	-17.3	%	
Maximum Fluid Level Velocity	0.05	in./s		Settling Time	61.5	s	
Number of Overshoots	1				1.0	min	
Control System Settings Optimized?	No			Steady-State Error	0.59	%	
Flow Rate Data Analysis							
Initial Return Line Flow Rate	20.8	gpm		Control Deadtime	2.9	s	
Time Flow Rate Ramp Initiated	546.4	s		Total Delay	6.4	s	
Minimum Flow Rate Pumped	13.90	gpm		Change From Initial	-33.2	%	
Final Return Line Flow Rate	16.80	gpm		Flow Rate	-19.2	%	
Expected Flow Rate Range	17.0	gpm		Theoretical Flow Rate	16.4	gpm	
	15.8	gpm		Flow Rate Accuracy	97.6	%	

4.4.3 Test #14 – Flow Rate Decrease

The pump, butterfly valve (#6 position), and 4.4 gpm hose were used to create a constant flow rate of 21.3 ±0.6 gpm. At time 205.0 s the total flow rate was decreased by 4.4 gpm. See Figure 4.11 for the LabVIEW results of Test #14.

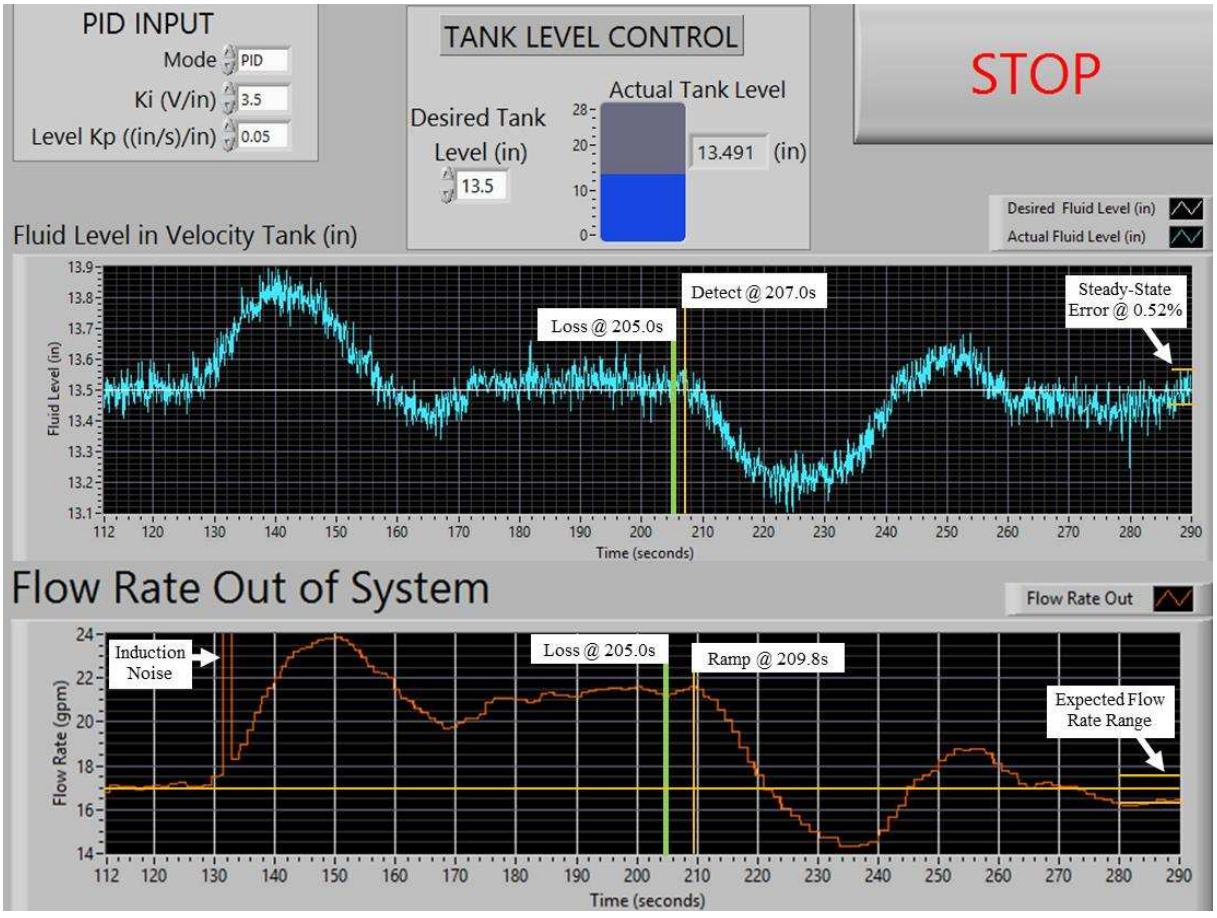

Figure 4.11 Test #14 fluid level and flow rate reaction in LabVIEW.

The level delay was 2.0 s after 4.4 gpm of flow was removed from the system. The flow rate determined in LabVIEW decreased from 21.3 gpm to the minimum flow rate of 14.4 gpm until the flow rate entering the velocity tank could increase the fluid level. The expected flow rate after removing the 4.4 gpm flow rate from the initial 21.3 gpm should fall between 16.3 gpm and 17.5 gpm. The final average flow rate determined was 16.5 gpm and falls within the expected range. See Table 4.11 for a detailed summary of the results compiled from Test #14. The results identified from Test #14 identify that controller system settings were not optimized since the controller overshot the target level, resulting in a settling time of 81.0 s. The flow rate

accuracy for Test #14 is 97.6%.

Table 4.11 Test #14: Summary of Results

Summary of Results: Test #14								
Initial System Parameters								
Initial Fluid Level (in.)	Initial Flow Rate (gpm)	Control System Settings		Ki (V/in.)	3.5			
13.5	21.3 ± 0.6			Level Kp ((in./s)in.)	0.05			
Test Design								
Test Type	Fixed Flow Rate loss of -4.4 gpm							
Method Removed	Fixed pressure hose from sink (cold) immediate shut off							
Time Removed	at 205.0 s for the remainder of the test							
Test Results								
Fluid Level Data Analysis								
Time Fluid Level Change Identified	207.0	s		Level Delay	2.0	s		
Min Mean Fluid Level	13.22	in.		Change	-0.28	in.		
Time to Reach Steady-State Error	288.0	s		Overshoot	-12.7	%		
Maximum Fluid Level Velocity	0.05	in./s		Settling Time	81.0	s		
Number of Overshoots	1				1.4	min		
Control System Settings Optimized?	No			Steady-State Error	0.52	%		
Flow Rate Data Analysis								
Initial Return Line Flow Rate	21.3	gpm		Control Deadtime	2.8	s		
Time Flow Rate Ramp Initiated	209.8	s		Total Delay	4.8	s		
Minimum Flow Rate Pumped	14.40	gpm		Change From Initial	-32.4	%		
Final Return Line Flow Rate	16.50	gpm		Flow Rate	-22.5	%		
Expected Flow Rate Range	17.5	gpm		Theoretical Flow Rate	16.9	gpm		
	16.3	gpm		Flow Rate Accuracy	97.6	%		

The PI control behavior is much less aggressive when flow rate decreases compared to the aggressive behavior when flow rate increases. This behavior identifies asymmetry in controller behavior based on the increase or decrease in flow rate.

4.5 Slowly Increasing Flow Rate Influx

It is important to identify how the system reacts to a realistic simulation involving an influx where the flow rate gradually increases. This test best represents an influx experienced

during normal drilling operations. When the system identifies a baseline flow rate, the return flow rate is slowly increased over a period between 60.0 s and 120.0 s. The control system and PCP conclude the test once the new return flow rate is identified.

4.5.1 Test #9 – Increasing Flow Rate Influx

The pump, butterfly valve (#6 position) were used to create a constant flow rate of 16.0 ±0.8 gpm. The return flow rate began to slowly increase at time 820.0 s and continued to increase to until the influx flow rate reached a peak rate gain of 4.4 gpm at time 900.0 s. See Figure 4.12 for the LabVIEW results of Test #9.

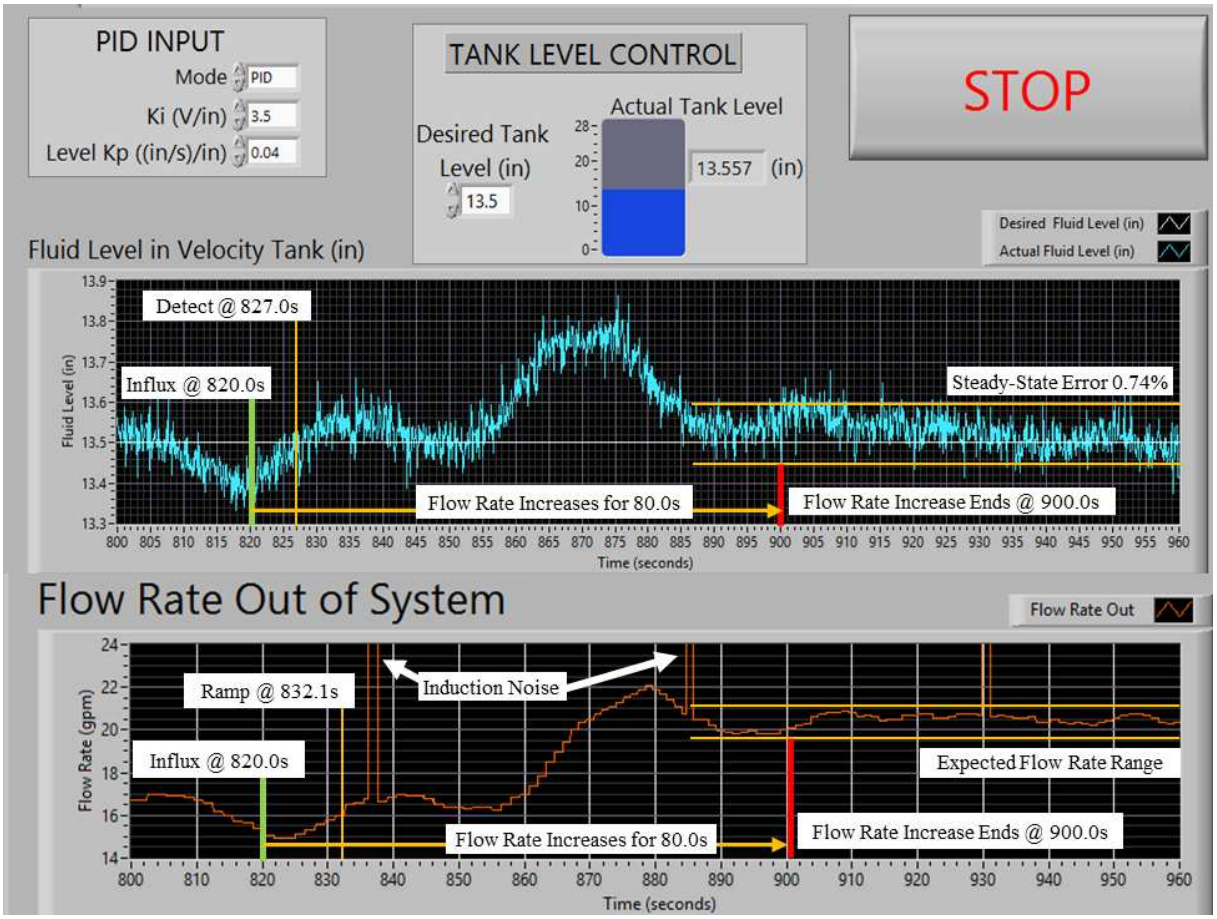

Figure 4.12 Test #9 fluid level and flow rate reaction in LabVIEW.

The VFR Meter identified an increase in return flow rate 7.0 s after an increase in flow rate was introduced at the baffles. The baseline flow rate increased from 16.0 ±0.8 gpm to a peak pump rate of 22.0 gpm to mitigate the extra fluid above the target level. The VFR Meter reached steady-state error within a settling time of 59.5 s and actively identified the new return flow rate

of 20.6 ±0.7 gpm before the influx flow rate peaked at 4.4 gpm. See Table 4.12 for a detailed summary of the test results compiled from Test #9.

Table 4.12 Test #9: Summary of Results

Summary of Results: Test #9							
Initial System Parameters							
Initial Fluid Level (in.)	Initial Flow Rate (gpm)	Control System Settings		Ki (V/in.)	3.5		
13.5	16.0 ± 0.8			Level Kp ((in./s)in.)	0.04		
Test Design							
Test Type	Steadily increasing Flow Rate influx of 4.4 gpm over 80.0 s						
Method Added	Fixed pressure hose from sink cold slowly turned on over 80.0 s						
Time Flow Increased	at 820.0 s until 900.0 s for remainder of the test						
Test Results							
Fluid Level Data Analysis							
Time Fluid Level Change Identified	827.0	s		Level Delay	7.0	s	
Max Mean Fluid Level	13.8	in.		Change	0.25	in.	
Time to Reach Steady-State Error	887	s		Overshoot	6.9	%	
Maximum Fluid Level Velocity	0.06	in./s		Settling Time	59.5	s	
Number of Overshoots	0				1.0	min	
Control System Settings Optimized?	Yes			Steady-State Error	0.74	%	
Flow Rate Data Analysis							
Initial Return Line Flow Rate	16.0	gpm		Control Deadtime	5.1	s	
Time Flow Rate Ramp Initiated	832.1	s		Total Delay	12.1	s	
Maximum Flow Rate Pumped	22.02	gpm		Change From Initial Flow Rate	37.6	%	
Final Return Line Flow Rate	20.60	gpm			28.8	%	
Expected Flow Rate Range	21.2	gpm		Theoretical Flow Rate	20.4	gpm	
	19.6	gpm		Flow Rate Accuracy	99.0	%	

The results from Test #9 identify optimized controller system settings, resulting in 99.0% flow rate accuracy.

4.5.2 Test #10 – Increasing Flow Rate Influx

The pump, butterfly valve (#6 position) were used to create a constant flow rate of 13.0 ±0.9 gpm. The return flow rate began to slowly increase at time 440.0 s and continued to increase to until the influx flow rate reached a peak rate gain of 4.4 gpm at time 500.0 s. See Figure 4.13 for the LabVIEW results of Test #10.

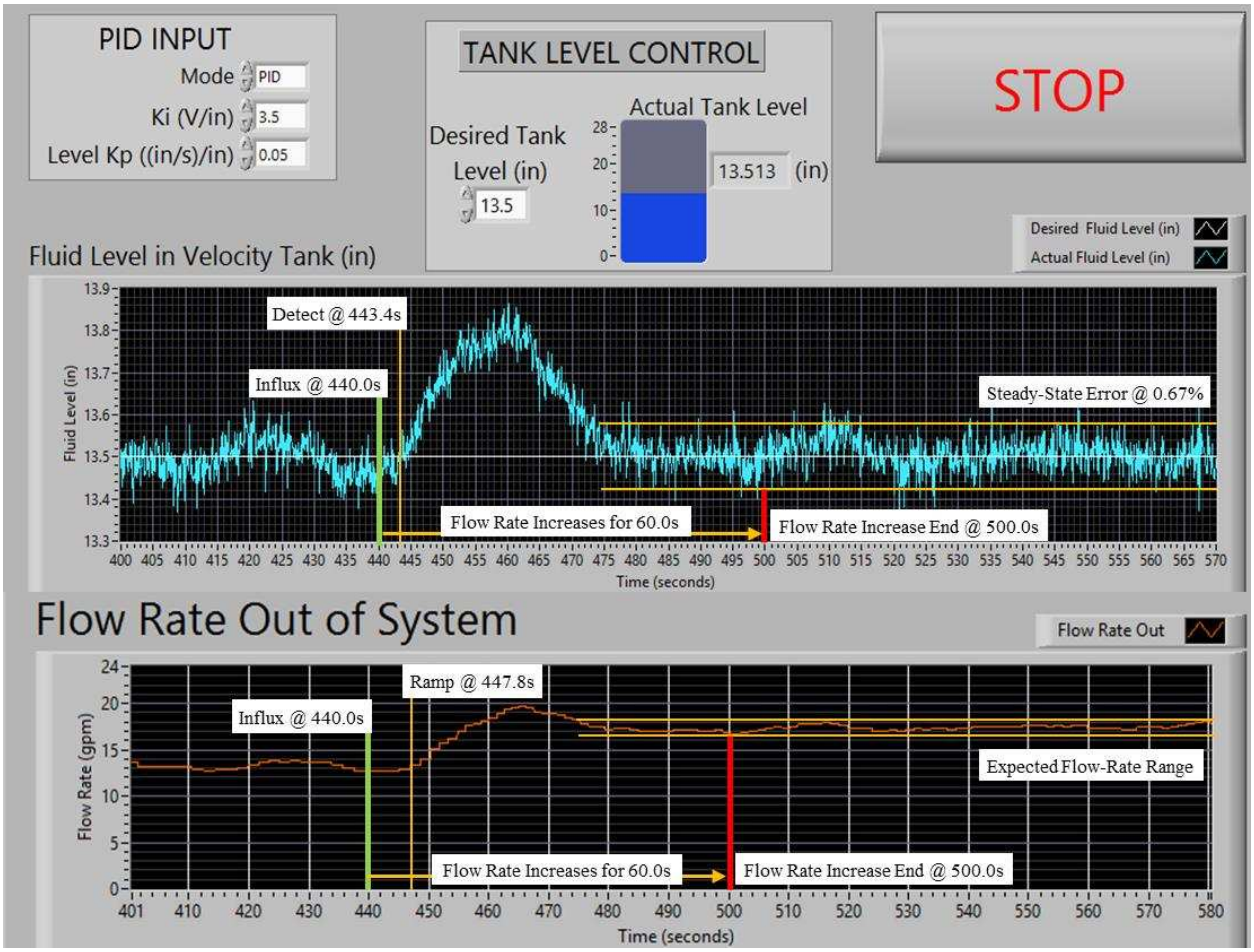

Figure 4.13 Test #10 fluid level and flow rate reaction in LabVIEW.

The VFR Meter identified an increase in return flow rate 3.4 s after an increase in flow rate was introduced at the baffles. The baseline flow rate increased from 13.0 ±0.9 gpm to a peak pump rate of 19.7 gpm to mitigate the extra fluid above the target level. The VFR Meter reached steady-state error within a settling time of 31.6 s and actively identified the new return flow rate of 17.5 ±0.4 gpm before the influx flow rate peaked at 4.4 gpm. See Table 4.13 for a detailed summary of the results compiled from Test #10. Test #10 results identify optimized controller settings during the 4.4 gpm influx increased over 60.0 s, resulting in 99.4% flow rate accuracy.

Table 4.13 Test #10: Summary of Results

Summary of Results: Test #10							
Initial System Parameters							
Initial Fluid Level (in.)	Initial Flow Rate (gpm)	Control System Settings		Ki (V/in.)	3.5		
13.5	13.0 ± 0.9			Level Kp ((in./s)in.)	0.05		
Test Design							
Test Type	Steadily increasing Flow Rate influx of 4.4 gpm over 60.0 s						
Method Added	Fixed pressure hose from sink cold slowly turned on over 60.0 s						
Time Flow Increased	at 440.0 s until 500.0 s for remainder of the test						
Test Results							
Fluid Level Data Analysis							
Time Fluid Level Change Identified	443.4	s		Level Delay	3.4	s	
Max Mean Fluid Level	13.8	in.		Change	0.30	in.	
Time to Reach Steady-State Error	475.0	s		Overshoot	12.6	%	
Maximum Fluid Level Velocity	0.06	in./s		Settling Time	31.6	s	
Number of Overshoots	0				0.5	min	
Control System Settings Optimized?	Yes			Steady-State Error	0.67	%	
Flow Rate Data Analysis							
Initial Return Line Flow Rate	13.0	gpm		Control Deadtime	4.4	s	
Time Flow Rate Ramp Initiated	447.8	s		Total Delay	7.8	s	
Maximum Flow Rate Pumped	19.70	gpm		Change From Initial Flow Rate	51.5	%	
Final Return Line Flow Rate	17.50	gpm			34.6	%	
Expected Flow Rate Range	18.3	gpm		Theoretical Flow Rate	17.4	gpm	
	16.5	gpm		Flow Rate Accuracy	99.4	%	

4.5.3 Test #11 – Increasing Flow Rate Influx

The pump, butterfly valve (#6 position) were used to create a constant flow rate of 17.5 ±0.8 gpm. The return flow rate began to slowly increase at time 410.0 s and continued to increase to until the influx flow rate reached a peak rate gain of 4.4 gpm at time 470.0 s. See Figure 4.14 for the LabVIEW results of Test #11.

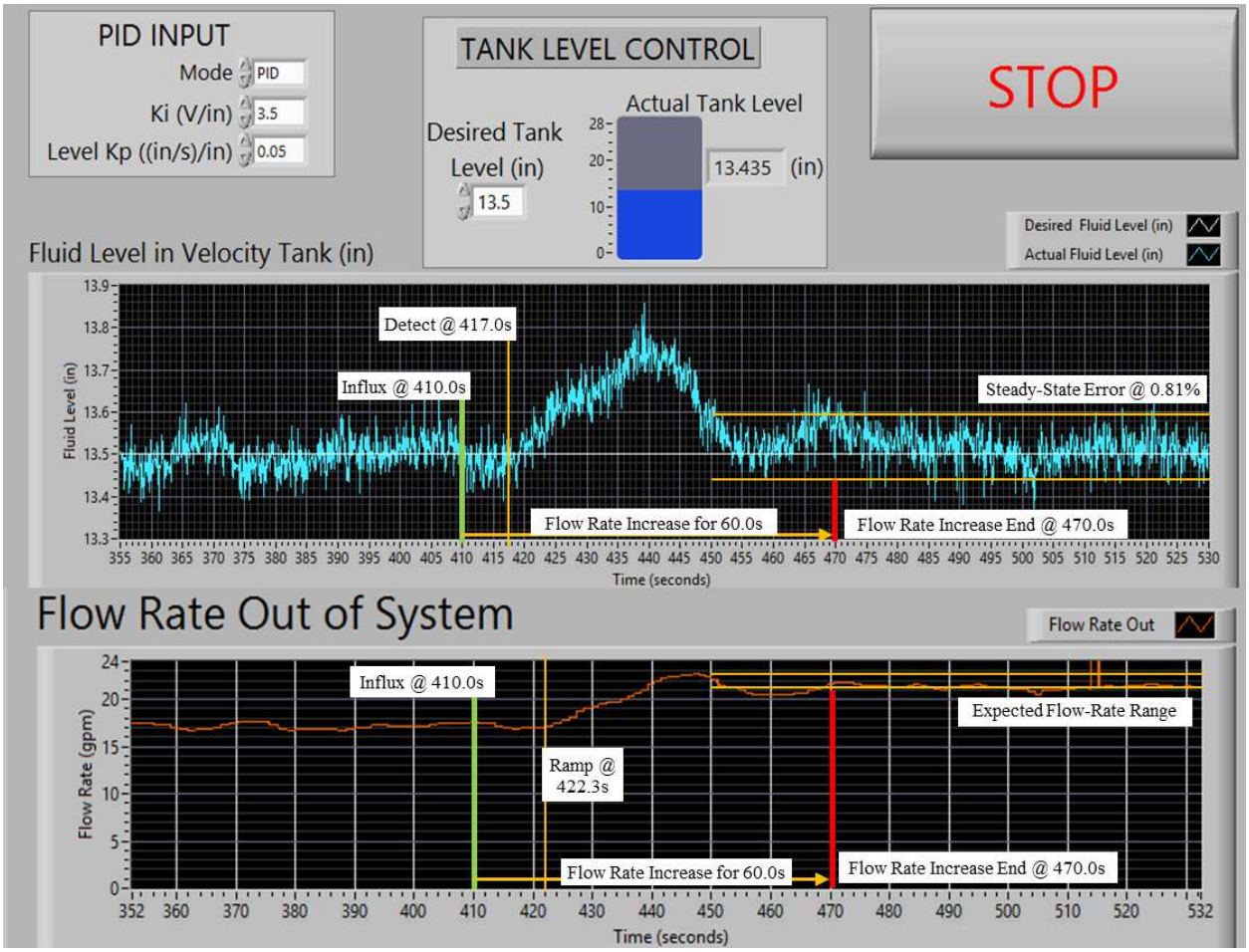

Figure 4.14 Test #11 fluid level and flow rate reaction in LabVIEW.

The VFR Meter identified an increase in return flow rate 7.0 s after an increase in flow rate was introduced at the baffles. The baseline flow rate increased from 17.5 ±0.8 gpm to a peak pump rate of 22.7 gpm to mitigate the extra fluid above the target level. The VFR Meter reached steady-state error within a settling time of 33.0 s and actively identified the new return flow rate of 21.4 ±0.9 gpm before the influx flow rate peaked at 4.4 gpm. See Table 4.14 for a detailed summary of the test results compiled from Test #11. The results identified from Test #11 identify that controller system settings were optimized during the 4.4 gpm flow rate increasing influx over 60.0 s, result in 97.7% flow rate accuracy.

Table 4.14 Test #11: Summary of Results

Summary of Results: Test #11							
Initial System Parameters							
Initial Fluid Level (in.)	Initial Flow Rate (gpm)	Control System Settings		Ki (V/in.)	3.5		
13.5	17.5 ± 0.8			Level Kp ((in./s)in.)	0.05		
Test Design							
Test Type	Steadily increasing Flow Rate influx of 4.4 gpm over 60.0 s						
Method Added	Fixed pressure hose from sink cold slowly turned on over 60.0 s						
Time Flow Increased	at 410.0 s until 470.0 s for remainder of the test						
Test Results							
Fluid Level Data Analysis							
Time Fluid Level Change Identified	417.0	s		Level Delay	7.0	s	
Max Mean Fluid Level	13.8	in.		Change	0.25	in.	
Time to Reach Steady-State Error	450.0	s		Overshoot	6.1	%	
Maximum Fluid Level Velocity	0.07	in./s		Settling Time	33.0	s	
Number of Overshoots	0				0.6	min	
Control System Settings Optimized?	Yes			Steady-State Error	0.81	%	
Flow Rate Data Analysis							
Initial Return Line Flow Rate	17.5	gpm		Control Deadtime	5.3	s	
Time Flow Rate Ramp Initiated	422.3	s		Total Delay	12.3	s	
Maximum Flow Rate Pumped	22.70	gpm		Change From Initial	29.7	%	
Final Return Line Flow Rate	21.40	gpm		Flow Rate	22.3	%	
Expected Flow Rate Range	22.7	gpm		Theoretical Flow Rate	21.9	gpm	
	21.1	gpm		Flow Rate Accuracy	97.7	%	

4.5.4 Test #12 – Increasing Flow Rate Influx

The pump, butterfly valve (#6 position) were used to create a constant flow rate of 16.9 ±0.4 gpm. The return flow rate began to slowly increase at time 200.0 s and continued to increase to until the influx flow rate reached a peak rate gain of 4.4 gpm at time 320.0 s. See Figure 4.15 for the LabVIEW results of Test #12.

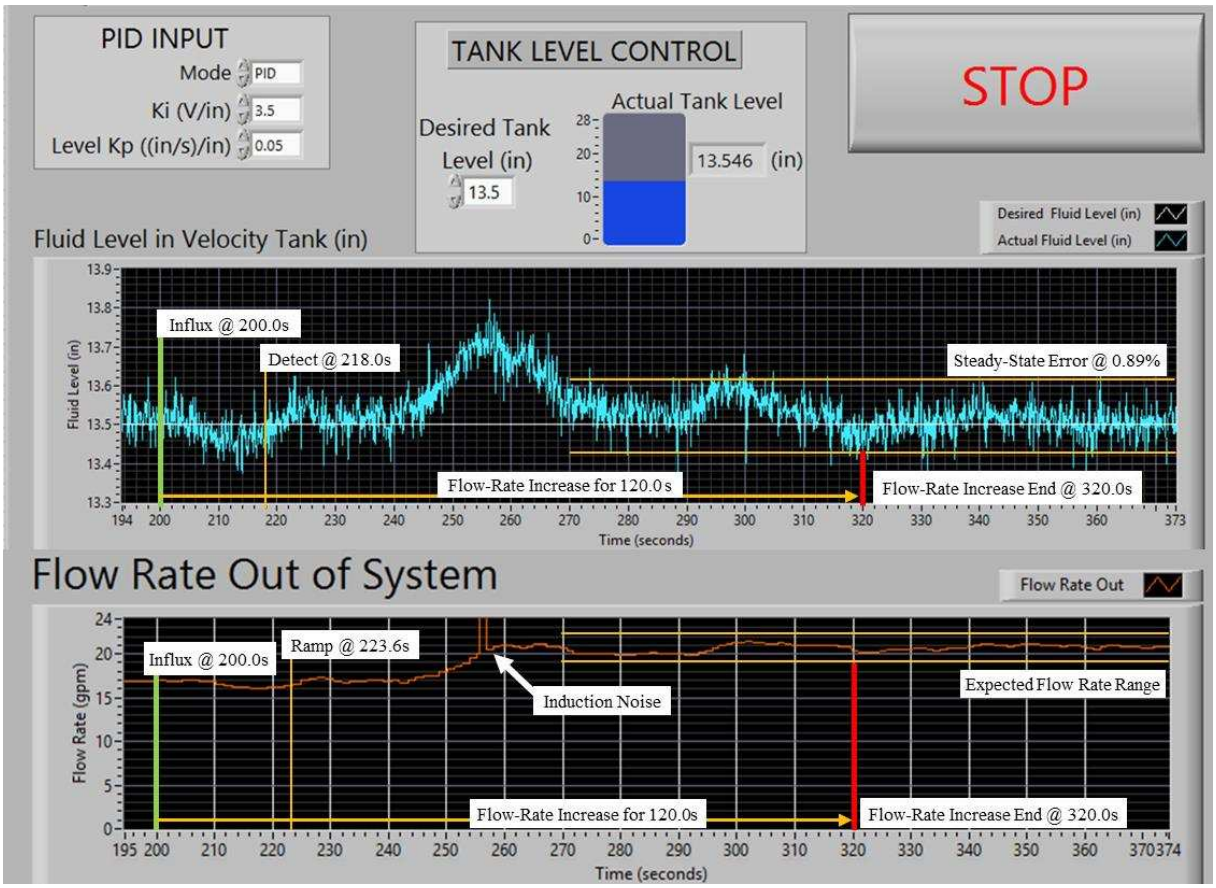

Figure 4.15 Test #12 fluid level and flow rate reaction in LabVIEW.

The VFR Meter identified an increase in return flow rate 18.0 s after an increase in flow rate was introduced at the baffles due to steady-state fluid level error. The baseline flow rate increased from 16.9 ±0.4 gpm to a peak pump rate of 21.6 gpm to mitigate the extra fluid above the target level. The VFR Meter reached steady-state error within a settling time of 52.0 s and actively identified the new return flow rate of 20.96 ±0.9 gpm before the influx flow rate peaked at 4.4 gpm. See Table 4.15 for a detailed summary of the test results compiled from Test #12.

The results identified from Test #12 identify that controller system settings were optimized

during the 4.4 gpm influx increased over 120.0 s, resulting in 98.4% flow rate accuracy.

Table 4.15 Test #12: Summary of Results

Summary of Results: Test #12							
Initial System Parameters							
Initial Fluid Level (in.)	Initial Flow Rate (gpm)	Control System Settings		Ki (V/in.)	3.5		
13.5	16.9 ± 0.4			Level Kp ((in./s)in.)	0.05		
Test Design							
Test Type	Steadily increasing Flow Rate influx of 4.4 gpm over 120.0 s						
Method Added	Fixed pressure hose from sink cold slowly turned on over 120.0 s						
Time Flow Increased	at 200.0 s until 320.0 s for remainder of the test						
Test Results							
Fluid Level Data Analysis							
Time Fluid Level Change Identified	218.0	s		Level Delay	18.0	s	
Max Mean Fluid Level	13.7	in.		Change	0.23	in.	
Time to Reach Steady-State Error	270.0	s		Overshoot	3.1	%	
Maximum Fluid Level Velocity	0.07	in./s		Settling Time	52.0	s	
Number of Overshoots	0				0.9	min	
Control System Settings Optimized?	Yes			Steady-State Error	0.89	%	
Flow Rate Data Analysis							
Initial Return Line Flow Rate	16.9	gpm		Control Deadtime	5.6	s	
Time Flow Rate Ramp Initiated	223.6	s		Total Delay	23.6	s	
Maximum Flow Rate Pumped	21.60	gpm		Change From Initial	27.8	%	
Final Return Line Flow Rate	20.96	gpm		Flow Rate	24.0	%	
Expected Flow Rate Range	21.7	gpm		Theoretical Flow Rate	21.3	gpm	
	20.9	gpm		Flow Rate Accuracy	98.4	%	

CHAPTER 5

DISCUSSION

As anticipated, the Active Control VFR Meter quickly detected each influx and then identified the new flow rate. Each test provided valuable insight used to define the VFR Meter response and controller behavior. Overall, the controller behaved as needed to rebalance the system after removing the excess fluid above the target level. The results from the thesis are to act as a benchmark for future system improvement. The results in this thesis reflect the controller and system design performance at the current time. Improvement of the current results based on controller logic and system design is desired and ideal but is outside the scope of this thesis.

This thesis required the identification of current system performance based on increasing and decreasing flow rate conditions. Determination of current system performance involved analysis of the fluid level and pump rate test results.

The combined results averaged for Test #4, Test #5, and Test #7 identified current system performance based on influx detection and increasing flow rate conditions. While Test #8, Test #13, and Test #14 identify current system performance for loss detection and decreasing flow rate conditions. The combined averages for Test #9, Test #10, Test #11, and Test #12 identify current system performance based on influx detection and slowly increasing flow rate conditions. This simulation represents the most common type of influx experienced on land drilling rigs. Next, the results of Test #6 will identify current system performance for multi-influx detection and multiple flow rate increases. Finally, fixed volume influx tests, Test #1, Test #2, and Test #3 are considered supplemental controlled tests for deterministic purposes. See Table 5.1 for the averaged results of all four test simulations conducted.

5.1 Influx Detection and Immediate Increase Flow Rate Conditions

Since the procedures of Test #4, Test #5, and Test #7 involves an immediate fixed flow rate influx for Simulation #2, the combined analysis best represented the system's standard performance to detect an immediate influx in flow rate. Settling time is an important indication of how quickly the system responds to change, including the time required to recover to a steady-state error. The PI controller and logic used to control system directly determines settling-time.

See Table 5.1 for the average test results and Figure 5.1 for the control response analysis.

Table 5.1 Averaged Results of Testing Simulations Conducted

Active Control VFR Meter Averaged Results		
Simulation #1: Single Fixed Volume Influx - Gradually Added		
Average Level Delay	6.4	s
Average Control Deadtime	4.5	s
Average Settling Time	83.0	s
Relative Flow Rate Accuracy	98.4	%
Simulation #2: Fixed Flow Rate Influx - Immediate Increase		
Average Level Delay	7.0	s
Average Control Deadtime	5.9	s
Average Settling Time	57.1	s
Relative Flow Rate Accuracy	98.9	%
Simulation #3: Fixed Flow Rate Loss - Immediate Reduction		
Average Level Delay	2.1	s
Average Control Deadtime	2.3	s
Average Settling Time	88.9	s
Relative Flow Rate Accuracy	98.1	%
Simulation #4: Increasing Flow Rate Influx - Slowly Introduced		
Average Level Delay	8.8	s
Average Control Deadtime	5.1	s
Average Settling Time	44.0	s
Relative Flow Rate Accuracy	98.6	%

Since the steady-state error is consistently (±0.1 in.) about the target-level, the average settling time for Test #4, Test #5, and Test #7 is 57.1 s. This resulted in the highest average relative flow rate accuracy of 98.9%. The shortest settling-time recorded is 38.0 s observed in Test #5. Ideally, the desired settling time is within seconds, but the further tuning of the control system is outside of the scope of this thesis. Controller logic recommendations are discussed in

Chapter 6. Next, deadtime analysis identified the delay in controller output response once the ultrasonic level sensor detected a change in fluid level. The average result of the deadtime for Test #4, Test #5, and Test #7 is 4.5 s. A 4.5 s deadtime or delay in response is not a significant amount of time on the rig but the deadtime adds to the total delay in the system's ability to detect an influx or loss. The average level delay is 7.0 s and the average total delay time is 13.0 s. This indicates the delay in PCP ramp rate once the return flow rate at the baffle changes.

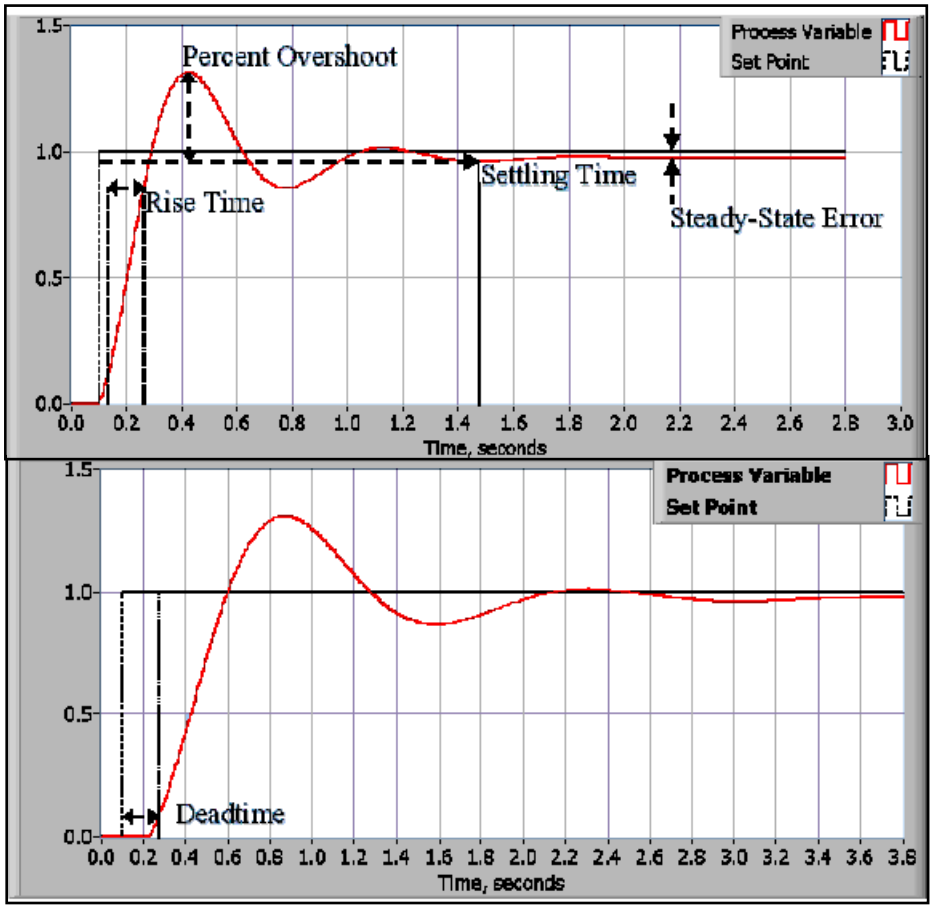

Figure 5.1 National Instruments (2011) PID analysis.

Percent overshoot analysis identified the dampening control the system, driven by the controller and gain settings. This occurs when the process variable (fluid level) crosses the set point, in this case, the target value. Undamped systems result in a high percentage of overshoot and increase settling time. High percent overshoot occurs when the proportional gain is set too high; this behavior is referred to as aggressiveness. A control system that uses a moderate gain setting should exhibit a shorter settling time than one with more aggressive gain settings. The

average result of percent overshoot for Test #4, Test #5, and Test #7 is 18.7%. Test #7's percent overshoot is 3.0%, which exhibits the smallest percent overshoot of all tests performed. Conversely, the shortest settling-time 38.0 s is observed in Test #5 and the percent overshoot is 22.7%. The percent change from initial flow rate clarifies this discrepancy in results. The percent change from initial flow rate is 99.7% in Test #5, compared to only 6.9% in Test #7.

The primary purpose of the volumetric flow meter is to measure the volumetric flow rate. Thus, the two most important factors to identify current system performance involve the level delay time and settling time. This is supported by the fact that it is the time where the flow-out equals flow in, therefore measuring the incoming volumetric flow rate. For this reason, level delay and settling time will exclusively identify current system performance as a means to more efficiently structure the remaining test interpretations.

5.2 Loss Detection and Decreasing Flow Rate Conditions

The procedure of Test #8, Test #13, and Test #14 involved an immediate reduction of a known fixed flow rate. The results define current system performance for loss detection and decreasing flow rate conditions. As mentioned in the previous section, the two most important defining parameters are a level delay and settling-time. The average level delay time for Simulation #3 is 2.1 s and the total delay is 4.4 s. The 0.0 s level delay recorded in Test #8 is not an accurate representation of the actual level delay. It is impossible to have a delay time of 0.0 s because that would require the Active Control VFR Meter to possess predictive capabilities. The explanation of Test #8 recording a level delay of 0.0 s is due to cyclic steady-state error observed in Figure 4.9. Just as the steady-state error peaked, the return flow rate decreased. The result of the behavior analyzed falsely represented the reported level delay time. Settling time is an important indication of how quickly the system responds to change, however, the average settling time identified for Test #8, Test #13, and Test #14 is was the longest at 88.9 s.

Asymmetric controller behavior was identified when the system flow rate decreased when compared to the behavior to when flow rate increases. The difference in system behavior directly influences settling time and the system's ability to determine VFR out is equal to the return VFR. The VFR Meter cannot handle losses as efficiently because the controller cannot control the rate at which water fills the tank when an overshoot occurs. Since the pump can only remove water from the tank, it must rely on the rate on return flow to keep the fluid level at the target level.

Overshoot occurs because when the deadtime results in the pump over displacing fluid as it continues to pump at the same rate. This resulted in 98.1% average flow rate accuracy, the lowest of any simulation type tested. A control type with a shorter deadtime would improve response time during a loss and reduce deadtime.

5.3 Influx Detection and Slow Increased Flow Rate Conditions

The averaged results of Test #9, Test #10, Test #11 and Test #12, identify that Simulation #4 exhibited the lowest average settling time in the study and a relative flow rate accuracy of 98.6%. Consequently, the averages also identify that Simulation #4 also indicated the longest total delay. These two very different results implicate unique controller behavior in Simulation #4. For a series of tests to have the greatest level delay (8.8 s) and the greatest average total delay (14.0 s) despite having the shortest settling time or 44.0 s. For this outcome to occur, the controller settings must be optimally tuned with cyclic steady-state error negatively affecting the level delay time. Had the total delay been less, each test would have reached the settling time sooner. Aside from appropriate controller tuning, the maximum mean fluid level was less than the other dynamic simulations. This shows that the increase in flow rate over time, allows the controller efficiency to improve because the ramp time is able to catch up to the increase in return flow rate. Since a shorter settling time allows for faster determination of return flow rate, action may be taken sooner. For an influx, this may involve enacting a shut in procedure and for a loss event, it may involve adding loss circulation material (LCM). Action taken sooner may reduce the criticality of the incident. Shutting in the well would stop additional influx, thus reducing the time required to circulate the kick out of the well. Adding LCM sooner in a loss event would reduce the amount of total fluid lost. Either incident results in the reduction of operational costs and non-productive time.

5.4 Two Separate Fixed Influx Added

The results of Test #6 (see Figure 4.7), identify the current system performance for multi-influx detection and multiple flow rate increases. This test was performed to determine how the system would react to a second influx after observing a max fluid level and gpm output. The test was carried out with a 53.0 s pause between each influx, clearly identify each influx response in RPM before returning to the target level. The fluid level hovered above the target level due to a lower K_p (0.02), but the reaction of each peak was expected. The settling time after the second

influx was 115.0 s.

5.5 Fixed Volume Influx

The averaged results of Test #1, Test #2, and Test #3, identifies that the Active Control VFR Meter is capable of quickly identifying a small fixed volume influx of fluid that would otherwise be missed. This occurs during normal drilling operations while tripping. Small volumes of influx can enter the well while tripping. Over time, the accumulation of each smaller influx can reduce the equivalent fluid density, leading to additional influx into the wellbore.

5.6 Sensor Response Time

The Active Control VFR Meter reaction time to changing flow rates is the most critical response in the system for several reasons. First, faster sensor response promotes a higher level of confidence in identifying the moment an influx/loss event occurred. Second, a faster sensor can react sooner to simultaneous changes in the system with less delay. The two significant sources of delay identified in the data analysis involve the level sensing delay and the control deadtime. Level sensor delay occurs because the fluid level measured by the ultrasonic sensor does not change the instant flow rate at the baffles changes. The fluid level change at the baffles must equalize with the fluid in the velocity tank before the shielded ultrasonic sensor can detect a fluid level change. Theoretically, the level sensing delay should have been a linear or proportionate response to the influx flow rate since the fluid has to travel the same distance between the baffle and ultrasonic sensor. Interestingly, a linear trend did not exist between flow rate and fluid level delay. The deviation from the expected linear trend is explained by the fluid level variation observed in steady-state error. Fluctuation in fluid level (±0.1 in.) observed within steady-state error conceals the exact time fluid level changes at the ultrasonic sensor. Chapter 6 discusses recommendations that address the improvement of sensor response time.

5.7 Calculated Return Flow Rate

The Active Control VFR Meter can only identify the return flow rate when the fluid level velocity is in the steady-state. However, a calculated flow rate can identify the flow rate during transient periods until the fluid level velocity returns to the steady-state error. Excess sensor signal noise contaminates the real-time results of the calculated return flow rate. Smoothing the ultrasonic sensor output can reduce noise and improve the quality of the calculated VFR. The calculated return flow rate is identified at any point in time. The tests performed in this research

evaluated the flow rate during the transient time (calculated VFR) but was not used to evaluate the Active Control VFR Meter behavior due to excessive noise. The excessive noise originated at the ultrasonic sensor and transferred to fluid level velocity, the rate of accumulation, and return flow rate in gpm. The calculated return flow rate is shown in Figure 5.2 as, "Calc Flow Rate In."

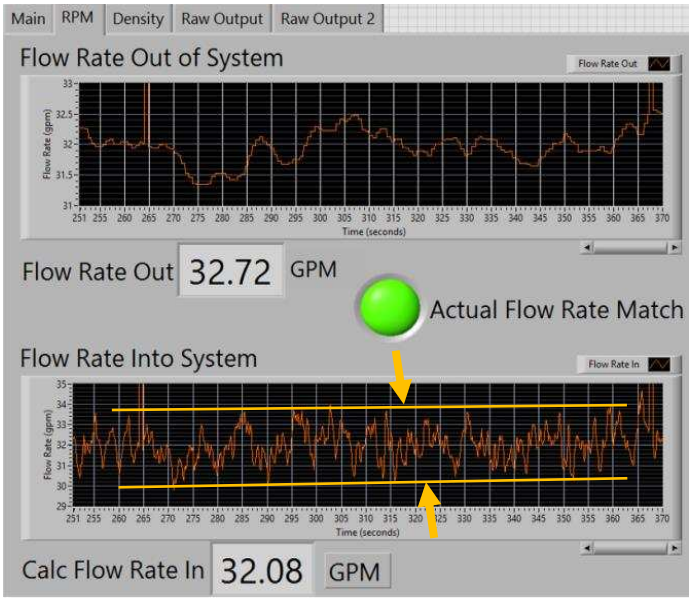

Figure 5.2 LabVIEW dashboard identifying "Calc Flow Rate In" output.

5.8 Limitations

Limitations of the current small scale Active Control VFR Meter tested do not and should not reflect or infer the limitations of a field capable Active Control VFR Meter. The two types of limitations involved in this study involve principle limitations and system limitations. Principle limitations involve the boundary where the principle of mass continuity no longer applies to the Active Control VFR Meter. This boundary is identified at the point where the constant fluid level in the velocity tank no longer suffices as a consistent means to identify that the flow rate out is equal to the flow rate in. Behavior that would indicate this limitation would involve fluid level fluctuation outside of the expected steady-state error when the pump rate is manually set to match the return fluid flow rate. A situation where this may occur involves moderate to highly compressible fluids such as aerated drilling fluids or foam. Since multiphase fluids were not tested at this point in the study, more research is required to identify a specific limit.

The small scale system limitations identified involve several mechanisms. The first limitation involves the ability to verify the VFR Meter's accuracy. A graduated beaker aided in

the calibration of a 5 gallon bucket used to measure fixed fluid amounts and flow rates using a stopwatch. Despite efforts to accurately identify the flow rates used and measured in this study, they were not certified by the national institute of standards. For this reason, all percent accuracy measurements identified are purely relative to the accuracy of the methods used to identify the flow rates in the lab.

The intent of this study included the calculation of fluid density at the Active Control VFR Meter to identify the fluid density before the shale shakers. However, the pressure transducer malfunction limited the ability to acquire the pressure necessary to calculate fluid density. This limitation is easily resolved with the installation of a new pressure sensor to facilitate the calculation of fluid density.

The induction proximity sensor used to identify RPM, limited the ability to measure RPM once every revolution. While this sufficed to successfully achieve the study objectives, it failed to provide reliable pump rotor position with accuracy below one revolution. This is important at slower RPM's especially when the LabVIEW program required a minimum of six RPM to avoid sensor timeout. This limitation is easily resolved with the installation of a rotary encoder. The level of accuracy associated with rotary encoders could provide feedback to the logic controller to improve system accuracy.

The ultrasonic sensor measurement of fluid level is limited by an accuracy of ±0.0625 in. Research costs dictated the use of an ultrasonic sensor despite the limitations previously known with current flow meter technology. Consequently, the ultrasonic sensor limitations involve environment parameters including density, temperature, and noise. Light Detection and Ranging (LIDAR) sensors using multi-wave optic sensors improve measurement resolution, accuracy, and extend the range of physical operating conditions.

CHAPTER 6

RECOMMENDATIONS

This Chapter identifies improvement for future tests, controller behavior, and hardware improvements in order of importance to system improvement and ease of implementation. Improvement of the Active Control VFD Meter apparatus and controller are crucial since continued development will commence within the next few months.

6.1 Noise Reduction

The current PI (proportional-integral) controller in the AC VFR Meter system is technically using PID (proportional-integral-derivative control) because the derivative "D" is taken at the fluid level. This fixes the derivative value but maintains control of the "P" and "I" gains tuning. The derivative of a complex signal such as the unfiltered fluid level signal is equal to the fluid level velocity. Figure 4.8 amplifies the steady-state error indicating that the low-pass filter did not filter noise adequately. Lipták (1998) discusses how PI controlled systems are prone to control signal saturation when the process transfer is the ratio of output to input of 1/s term. This type of ratio leads to reset windup and produces an unstable system near the steady-state because as Lipták (1998) explains, the integral continues to integrate the error. To improve the control quality, a moving average is necessary to reduce the noise and smooth the control signal before the control is sent to the VFD. See Figure 6.1 for the result of a moving average from the original signal noise.

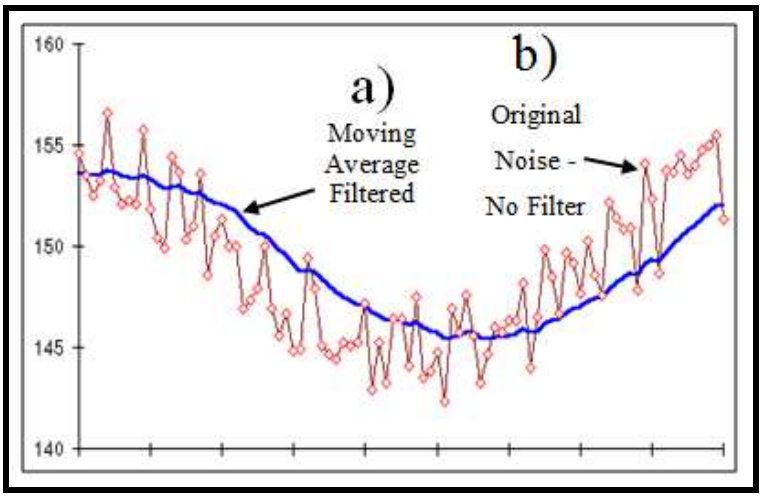

Figure 6.1 Walker (2017) shows that a moving average (a) reduces noise (b).

It is important to note that smoothing can cause distortion of data and create a misrepresentation of results. Additionally, there are different types of smoothing, and some cause more deadtime (delay in controller response). Error increases with the development of vibrations when fluid enters the velocity tank without sufficient baffling, the induction motor ramps excessively, or the ultrasonic sensor is attached to an undamped object. When a PI controller uses the signal from a noisy signal, the error amplifies and system instability increases. This is relevant when the fluid level velocity is calculated using the noisy fluid level. Thus, the slightest noise in fluid surface measured will produce a greater steady-state error for a calculated parameter. An improvement in fluid level quality should decrease noise and result in a faster detection time.

6.2 Controller Type

Further investigation into alternative control logic to improve this system include a PID autotuner, feedback in a feedforward system, lead-lag control (since ramp up and ramp down time of PCP is measured) or as NI (2017) suggests, a combination of control types used for different reasons that address PI control limitations (reset K_i at target level).

6.3 Sensor Quality

The pressure sensor exhibited the poorest performance of the sensors used. When powered, the sensor jumped to the expected fluid pressure but exhibited signal drop-off instability due to a negative voltage reading and possibly due to its large range (0-30 psig). The sensor was tested in water and air before and after multiple attempts to recalibrate the sensor. Since trapped air was a legitimate concern, all air was purged from the inlet of the sensor to eliminate trapped air interference with the sensing membrane, but the drop off error never improved.

The induction sensor also exhibited poor performance when properly wired and installed. With moderate rotor rotation (80 RPM) the frequently spiked for a single count in the 1000 RPM to 6000 RPM range before returning to 80 RPM on the next revolution. Since the maximum pump RPM allowed is less than 200 RPM, double count error was identified as the detection issue because the sensor detected a single probe count twice within 1/60 of a revolution. Sensor orientation and placement were varied without improvement in results. Since the rev/min is such a critical component of this research, an encoder should replace the current induction sensor. The ultrasonic sensor worked and could detect fluid levels within its declared 0.125 in. claimed

accuracy but produced excessive noise within the ±0.1 in. steady-state error identified. Therefore, the more advanced LIDAR sensor is recommended for use in future studies. Its accuracy, number of limitations, and reliability are a significant improvement compared to the ultrasonic sensor.

6.4 Motor Type

A synchronous motor was the ideal motor selected to drive a PCP. However, only an induction motor was available within the time frame for this research. Induction motors are known for their variability in rev/min when torque changes. A synchronous motor can deliver accurate and reliable RPM based on the frequency of the supplied voltage. Since synchronous motors are not self-starting, a secondary startup motor is required. Once the motor is running, a parasitic flow loop could supply the minimum continuous flow rate required to prevent unexpected pump shutdown when the return rate is near zero gpm. The constant flow rate, in addition to the return flow rate, is then deducted from the total flow rate pumped by the PCP. A synchronous motor should provide more stable flow rate readings than an induction motor because the motor RPM is independent of torque, the RPM is known using the frequency of a synchronous motor (verified with precision rotary encoder) indicating the actual flow rate pumped out of the velocity tank in gallons per minute.

CHAPTER 7

CONCLUSION

The continuation of the presented research can eventually lead to the state of the art development of Active Control Volumetric Flow Rate Meter. The successful study of objectives achieved in this research will serve as a base for planning future research already underway. First, the volumetric flow rate meter demonstrated the principle of mass continuity as the volumetric flow rate was successful measured in each dynamic test type performed. Second, the VFR Meter behavior quantified in dynamic simulations includes; influx/loss detection times, relative flow rate accuracy, comprehensive controller analysis, and delay in system response. Third, identification of the actions required to improve VFR Meter performance includes higher quality sensors, automated controller integration, enhanced logic, improved signal conditioning methods, noise reduction, and improvement in RPM stability with the use of a synchronous motor.

The current prototype works autonomously and functions as intended to prove the initial concept of a volumetric flow rate detection and determination. The initial results concluded that the Active Control VFR Meter could identify an influx or loss in less than 5.0 s and determine the volumetric flow rate within 36.0 s. With several basic improvements, the system will have greater accuracy, more sensitive instruments, ability to calculate density and a high-performance controller. Plans to quantify the accuracy and improve the VFR Meter performance have already begun.

An Active Control VFR Meter with unmatched precision, reliability, and unique flexibility would stand alone in its own class of automated volumetric flow meters. Since the reliability of current return flow rates are largely understood as, determination of true volumetric flow rates could offer a look at how far off the current technology is from inferring volumetric flow rate from sensor measurements as Cadillac Meter (2017) argues. The VFR Meter could also act as a new method for verification or determination of onsite flow meter assurance for field operating in line flow rate meters. This concept allows a land rig to request flow rate verification of existing in-line flow sensor equipment. This verification would allow current rigs to test a first in its class AC VFR Meter to learn how far off calibration the rig sensors are from indicating the

true volumetric flow rate. The suggestion of this method of implementation new technology addresses the skeptical nature associated with new technology in the industry. It would allow the industry to an opportunity to see the improvement in flow rate determination where other flow meters have failed in the past. Eventually, a skid mounted full-scale unit will put the VFR Meter to work on location under the harshest conditions 24/7, 365 days a year.

Now that the small scale, proof of concept has validity, more research and development of the Active Control VFR Meter is required. Since the initial research has proven itself successful in measuring VFR the next steps will eventually demonstrate the value added to operations using an Active Control VFR Meter on their location.

REFERENCES

Adrian. 2015. Mud Circulation Equipment. *Ghost Pool*, 16 March 2015, http://www.Ekomeri.Com/Mud-Circulation-Equipment/ (accessed 2 April 2017).

Ahmed, M. A., Hegab, O. A., and Sabry, A. 2015. Early Detection Enhancement Of The Kick And Near Balance Drilling Using Mud Logging Warning Sign. Egyptian Journal of Basic and Applied Sciences 3 (1): 85–93. (16 September 2015 revision), https://doi.org/10.1016/j.ejbas.2015.09.006 (accessed 9 January 2017).

Avery, P. 2017. Introduction To Pid Control. *Machine Design*, 01 March 2009, http://www.Machinedesign.Com/Sensors/Introduction-Pid-Control?Utm_Test=Redirect&Utm_Referrer=https://www.google.com/ (accessed 1 January 2017).

Cadillac Meter. 2017. Flow Meter Calibration Is A Thing Of The Past With The New Industry Standard, http://Cadillacmeter.com/Flow-Meter-Calibration/ (accessed 14 April 2017).

Control Guru. 2017. Comparing Controller Performance Using Plot Data, http://www.Controlguru.Com/Comparing-Controller-Performance-Using-Plot-Data/ (accessed 20 March 2017).

Control Guru. 2017. Using Signal Filters In Our PID Loop, http://www.Controlguru.com/Using-Signal-Filters-In-Our-Pid-Loop/ (accessed 20 March 2017).

Emerson. 2017. Coriolis Measurement: Part 2. *Flow Solutions Blog,* http://www.Flowsolutionsblog.com/The-Basics-Of-Flow-Measurement-With-Coriolis-Meters-Part-2/ (accessed 3 February 2017).

Flow Solutions Blog. 2016. The Basics Of Flow Measurement With Coriolis Meters Part 2, December 2016, http://www.Flowsolutionsblog.com/The-Basics-of-Flow-Measurement-With-Coriolis-Meters-Part-2/ (accessed 15 January 2017).

Fraser, A., Lindley, R., Moore, D. et al. 2014. Early Kick Detection Methods and Technologies. Presented at the SPE Annual Technical Conference and Exhibition held in Amsterdam, The Netherlands, 27-29 October. SPE-170756-MS. http://dx.doi.org/10.2118/170756-MS (accessed 19 February 2017).

Lipták, B. G. 1999. Control Theory. Instrumentation Engineers' Handbook, third edition. Chap. 1, 1-159. Boca Raton, Florida: CRC Press LLC.

Livelli, G. 2010. Flowmeter Piping Requirements. Flow Control Network, 26 September 2010, http://www.Flowcontrolnetwork.com/Flowmeter-Piping-Requirements/ (accessed 14 April 2017).

National Instruments. 2011. PID Theory Explained, 29 March 2011, http://www.Ni.com/White-Paper/3782/En/ (accessed 14 April 2017).

Norman, J. 2011. Coriolis Sensors Open Lines To Real-Time Data. Drilling Contractor, 21 September 2011, http://www.Drillingcontractor.Org/Coriolis-Sensors-Open-Lines-To-Real-Time-Data-10682 (accessed 20 March 2017).

Schafer, D. M., Loeppke, G. E., Glowka, D. A. et al. 1992. An Evaluation Of Flowmeters For The Detection Of Kicks And Lost Circulation During Drilling. SPE/ADC Drilling Conference held in New Orleans, Louisiana, 18-21 February. SPE-23935-MS. https://doi.org/10.2118/23935-MS (accessed 22 April 2017).

Speers, J. M. and Gehrig, G. F. 1987. Delta Flow: An Accurate, Reliable System For Detecting Kicks And Loss Of Circulation During Drilling. SPE Drilling Engineering 2 (04): 359-363. SPE-13496-PA. https://doi.org/10.2118/13496-Pa (accessed 5 March 2017).

Spitzer, D. 2010. Which Flowmeter Types Are Volumetric? Flow Control Network, 26 September 2010, http://www.Flowcontrolnetwork.Com/Which-Flowmeter-Types-Are-Volumetric/ (accessed 11 March 2017).

Walker, J. 2017. Signal And Noise (29 April 2017 update), Fourmilab, https://www.Fourmilab.Ch/Hackdiet/E4/Signalnoise.html (accessed 3 April 2017).

APPENDIX A

To perform this research, pumps, motors, drivers, sensors, tanks, PVC pipe, and fittings were specified and quoted. Equipment selected for this research includes a brief list of specifications and the reason it was selected. The initially quoted cost of the project was roughly $25,000 but the final cost of the project was closer to $12,000, thanks to Colorado School of Mines Facilities for several donations.

A.1 Pump and Motor

The pump was the main piece of equipment necessary to conduct this research. It was imperative that the pump was positive displacement type pump due to the volumetric nature of the requiring a constant fluid flow rate. Centripetal pumps and other non-volumetric pumps could not be used for this research due to the poor volumetric efficiency. The Seepex BN Range 17-6LS, 40 gpm progressive cavity pump was selected to run with a Nord 3 phase, 3.0 HP, 1710 RPM induction motor with a 9.8 gear train reduction.

Figure A.1 Seepex BN Range Standard PCP and induction motor.

Normal operating limits of the motor and pump range from 0 RPM 182 RPM. With 0.2 gallons per revolution pump factor only pumps 36.5 gpm of the initially desired 40 gpm at 60 Hz. This pump has a 4.0 in. vertical flanged intake and a 3.0 in. flange on the discharge side piped to the reserve tank.

A.2 VFD Controller

The TECO-Westinghouse E510 Variable Frequency Drive (VFD) was selected based on its ability to control the frequency for an induction motor and power capability. This particular VFD has a NEMA enclosure, 3 phase 230 VAC (208 V AC) with a 3 phase output to the motor with a resolution of 0.06 Hz accuracy.

a) b)

Figure A.2 TECO-Westinghouse E510 NEMA 3 Phase VFD: (a) Wall mounted with 3 phase 208 V AC installed and 20 A fast acting non-delay fuse installed to prevent a facility power surge from damaging the VFD; (b) NEMA enclosure plate removed to show inside of VFD.

See Figure A.3 for the wiring diagram identifying the proper schematic used to connect the VFD to the NI DAQ to control the frequency with voltage.

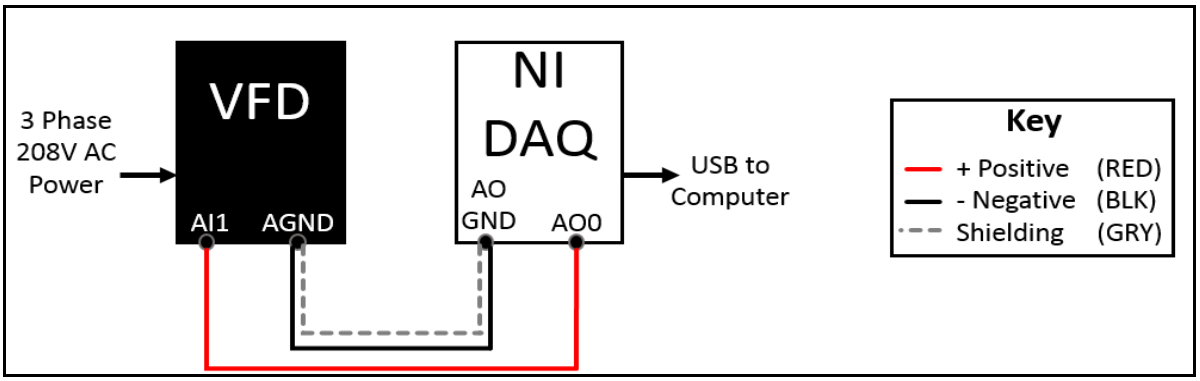

Figure A.3 Wiring schematic for the connection of the VFD to the NI DAQ.

A.3 Doublesphere Vibration Dampener

See Figure A.4 for visual of the Doublesphere vibration dampener. To feed the pump intake, a 4.0 in double flanged rubber double sphere expansion/vibration upward through the stack to the velocity tank to maintain a constant smooth, fluid level. Installing the spool above the pump intake dampens pump and motor vibrations traveling upward to the velocity tank. Dampening these vibrations above the pump is critical because vibrations can create wave action in the velocity tank and negatively affect the surface quality of the water. Wave action has a negative effect on the ultrasonic measurement of fluid level because the ultrasonic sensor samples fluid level proximity from the sensor 1000 times a second. This means that the sensor has the capability to sense the difference in height between the crest and trough with 0.019 in. of precision.

a) b)

Figure A.4 Metraflex 4.0 in. Doublesphere expansion joint: (a) with a ruler for scale; (b) installed Doublesphere on top of the Seepex PCP (knife valve PVC flange bolted to the upper Doublesphere flange).

The dampening system used in the velocity tank for this test will be discussed later, but the damped effect it produces represents the same result of desired surface flatness that the doublesphere accomplishes to maximize the accuracy of the ultrasonic sensor reading.

A.4 Knife Gate Valve

See Figure A.5 for visual of the knife valve. A knife valve was made up to the flange stack to stop the flow of water just below the velocity tank in the event of a catastrophic failure. The knife valve also allows complete isolation and draining of the lower system only make repairs if needed.

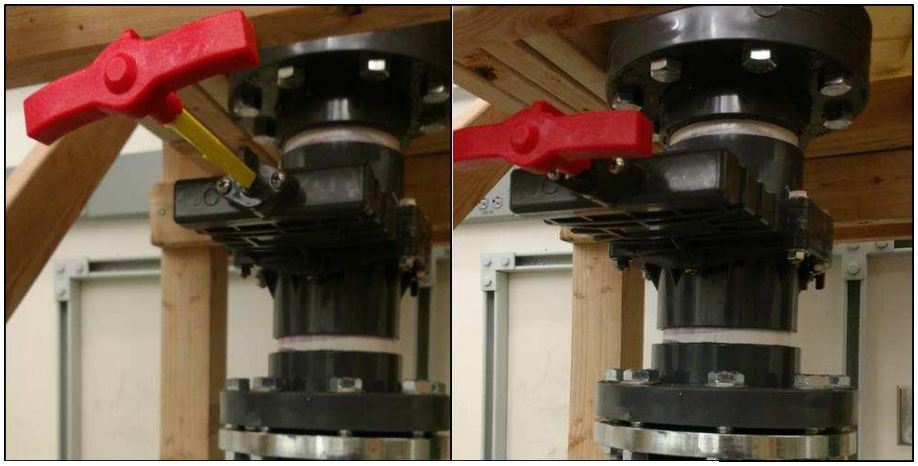

a) b)

Figure A.5 Socket by socket 4.0 in. knife gate valve: (a) valve open, indicated by the yellow safety snap bar; (b) valve closed, handle pushed all the way in flush with the valve body (no room for yellow safety bar).

A.5 Tank Bulkhead

The flanged tank bulkhead, seen in Figure A.6, connects the flange stack to the velocity tank. A gasket seals the flange connection, and all plastic flanges are properly torqued to 25 lbf/ft per ANSI specification. The bulkhead rubber gasket was Flex Seal welded (waterproofing spray glue) to the bulkhead connection to eliminate leak paths when connected to the bottom of the velocity tank. A 5.75 in to 5.78 in. hole was cut in the bottom of the plastic 53 gallon drum to allow the threaded portion of the bulkhead fitting to pass through the bottom of the tank. To install the bulkhead fitting, the bottom of the tank was sprayed with Flex Seal to form a watertight connection between the bottom of the tank and the top mating surface of the lower half of the bulkhead fitting.

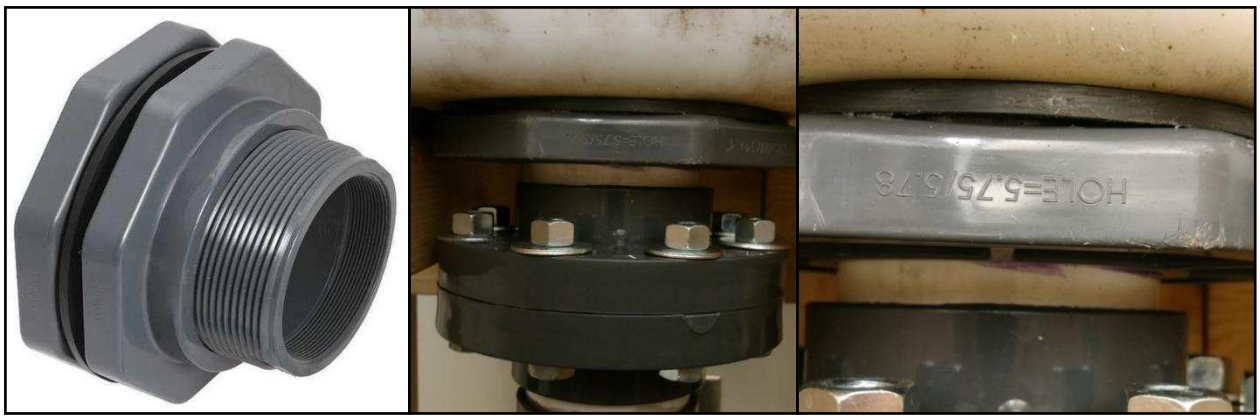

a) b) c)

Figure A.6 FNPT PVC 4.0 in. Bulkhead Tank Fitting: (a) Bulkhead components showing from left to right the 4.0 in. socket lower bulkhead half, the rubber gasket and the threaded upper bulkhead half; (b) bulkhead shown plastic welded to 4.0 in. PVC pipe and 4.0 in. PVC socket flange bolted and properly torqued to the ANSI 25 lbf/ft specifications; (c) close up of the Flex Seal surfaces sprayed to create sealed watertight surfaces on either side of the rubber gasket.

Ideally, the velocity tank would be a high angle cone bottom tank, for reasons discussed below, however, for proof of concept purposes it was not practical to order a cone bottom tank with a plastic welded flange added to the bottom of the tank because the lead time was too long, and it would have cost over $700 more than the recycled 53 gallon plastic drum from the Colorado School of Mines Facilities Department. See Figure A.6 for the bulkhead connection used with the 53 gallon tank. The reason a high angle cone bottom tank is an ideal shape for the velocity tank in the future for a quarter or half scale field trial build is that solids would have a difficult time settling on the bottom of the tank. If a flat bottom drum or shallow angle cone bottom tank were used, fines, cuttings, and solids could settle out on the bottom of the tank over time. This could cause pressure sensor errors, clogged PVC pipe leading to ultrasonic fluid level readings and solids building up, sliding into the stack, and then loading the pump with solids. If solids buildup is severe, it may even plug or damage the pump. This would result in the system overloading and may cause the pump to damage itself due to dry running. The velocity tank has one sensor monitoring fluid height and fluid pressure in the bottom of the tank.

A.6 Ultrasonic Sensor

A Flowline DX-10 EchoPod ultrasonic liquid sensor monitors the position of the fluid level inside of the velocity tank. The Flowline sensor has 1.0 in. NPT threads on the bottom of the sensor seen in Figure A.7 below. Flowline recommended using a 3.0 in. PVC pipe 2.0 in

minimum inside diameter (ID) as stated in the Flowline manual with a reducer and a 1.0 in. NPT adapter to shield the fluid level from wave action inside of the tank. It was important to drill holes towards the top of the 3.0 in. PVC to allow ample airflow in and out of the pipe as the fluid level falls and rises within the velocity tank. Not drilling holes or drilling holes that are too small may not provide sufficient cross-sectional airflow and can trap air inside. Fluid levels could flucuate unevenly by trapping pressure inside the pipe and indicate a lower than actual fluid height when the fluid level inside the velocity tank is increasing or create a vacuum inside of the pipe and indicate a higher than actual fluid height when the fluid level in the velocity tank is decreasing.

Figure A.7 Flowline Ultrasonic Sensor.

See Figure A.8 for the USB Flowline offers a USB with screw terminals that allows the sensor to directly to the USB and then directly connect to a computer's USB to run the sensor directly with free downloadable Flowline software.

Figure A.8 Flowline Fob for USB interfaces with screw terminals.

Since LabVIEW was selected as the programming software used for this test, it should be noted that the optional Flowline USB fob with screw terminals was not used because it is not compatible with LabVIEW but may be desired in unique non-programing circumstances. Since

the Flowline DX-10 ultrasonic sensor is 0-10 V DC analog output compatible it will communicate its signal with the LabVIEW software through the NI DAQ via USB. Figure A.9 depicts the wiring schematic for the Flowline ultrasonic sensor.

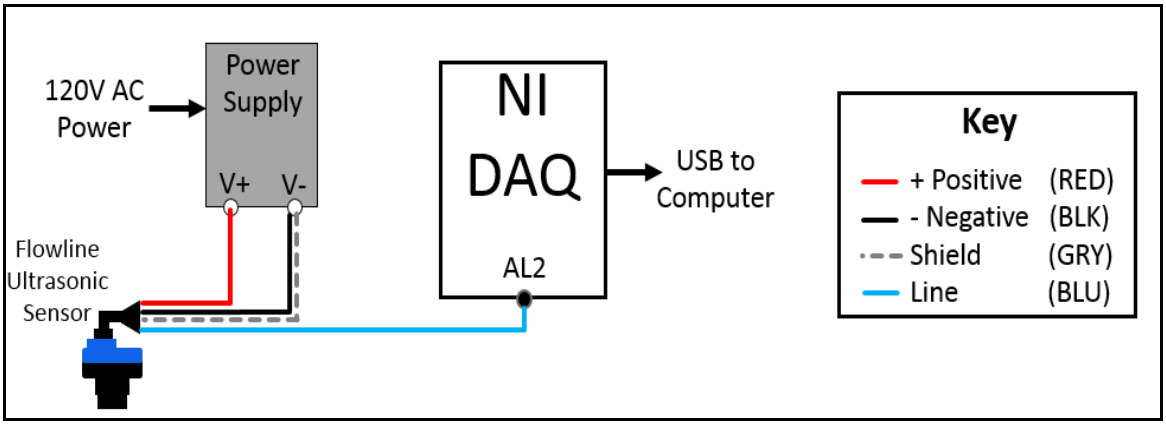

Figure A.9 Wiring diagram represents the proper way to wire the Flowline ultrasonic sensor to the 24 V DC power supply and connect it to the NI DAQ to determine fluid height with voltage.

A.7 National Instruments DAQ and LabVIEW

The NI DAQ, shown in Figure A.10, sends an analog output voltage to the NI BUS-Powered M Series DAQ USB 6212M with NI-DAQMX driver. The NI DAQ interprets voltage and sends the corresponding digital signal to the computer via USB. Furthermore, it possesses digital and analog input/output capabilities and provides ample room for additional sensors for future research.

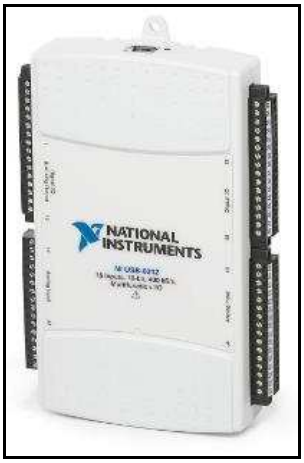

Figure A.10 Bus-Powered M Series Multifunctional DAQ for USB-16 Bit, up to 400 kS/s with up to 16 analog inputs and 16 digital I/O inputs.

LabVIEW correlates and converts the received voltage from the NI DAQ to represent the proper fluid height inside the velocity tank in units per inch. An offset indicated by the top of the blue line was used because the top of the bulkhead fitting inside the tank is roughly 4.5 in. high. This means that if the fluid level measured from the bottom of the tank is less than 4.5 in. then the pump can run dry once the fluid inside the 4.0 in. stack is pumped out of the tank. Since the fluid level in the tank should never drop below this level, the defined target-level corresponding to 0.0 in. is 4.5 in. off the bottom of the velocity tank. To prevent the fluid entering the intake in the bottom of the velocity tank from rotating, the tank was drained at maximum velocity to determine the proper offset from the newly established effective tank zero line to eliminate the introduction of air into the PCP. It should be noted that the pump could handle gas, liquid and solids at the same time without causing damage to the pump; however, severe rotational flow would create an error in velocity tank fluid level and pump factor due to the displaced liquid volume.

The minimum fluid level offset was found to be roughly 10.0 in. above the effective tank zero line and would prevent fluid from rotating inside of the velocity tank at maximum operating conditions. To enforce the 10.0 in. offset to ensure the tank will not empty past 10.0 in., a minimum lower tank level safety limit was set in the LabVIEW program to automatically stop the pump if the fluid level in the velocity tank drops to 10.0 in.

A.8 Power Supply

The Newstyle Power Supply, seen in Figure A.11, powers all of the sensors used in this study. This power supply is used in this research for its high performance and affordability.

Figure A.11 Newstyle 24 V, 15 A DC universal regulated switching power supply, 120 V AC 360 W.

A.9 Pressure Transmitter

The ProSense pressure transmitter shown in Figure A.12, has a 0 psig to 30 psig range and a 0 V to 10 V DC analog output. It was selected to measure the pressure at the bottom of the velocity tank with ±0.15 psig precision. This sensor was preferred over other pressure sensors because it was waterproof, the 0 psig to 30 psig range is surprisingly small, and 0-10 V DV sensors with a smaller pressure range are expensive and difficult to find. However, it is ideal if a waterproof sensor is available with a smaller pressure range, has a 0-10 V DC analog voltage range and is comparable in price.

Figure A.12 ProSense waterproof pressure transmitter, 0 psig to 30 psig range with 0-10 V DC analog output, 14 V to 36 V DC operating voltage.

Figure A.13 depicts the wiring schematic for the ProSense waterproof pressure transmitter.

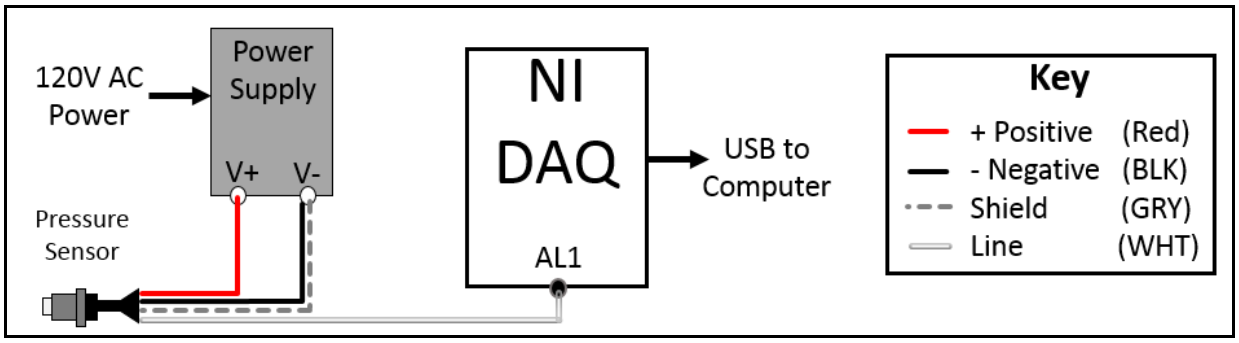

Figure A.13 Wiring diagram to represent the proper way to connect the ProSense waterproof Sensor to the 24 V DC power supply and connect it to the NI DAQ to determine bottom tank fluid pressure with voltage.

A.10 Inductive Proximity Sensor

Selected because of its digital and analog input/output capabilities and sufficient room for additional sensors desired for future testing. The proximity sensor shown in Figure A.14, reported the number of pump rotor rotations occurred in 60 seconds to determine the pump's RPM and flowrate out of the system.

Figure A.14 Inductive proximity sensor PNP, 7 mm (0.27 in.) nominal sensing distance with a 0-10 V DC analog output.

Figure A.15 depicts the wiring schematic for the inductive proximity sensor.

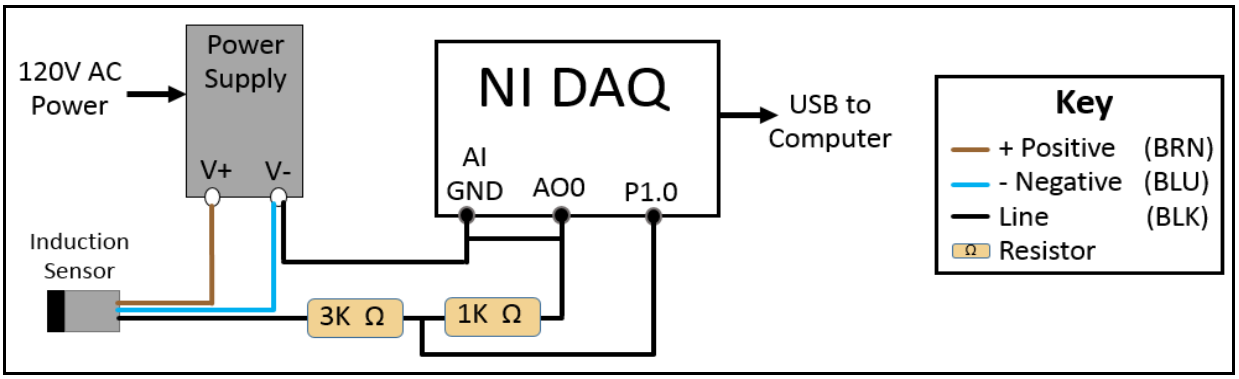

Figure A.15 Wiring diagram to represent the proper way to connect the inductive proximity sensor, PNP, with 7.0 mm nominal sensing distance unshielded to the 24 V DC power supply and connect it to the NI DAQ to determine the pump RPM with voltage.